Chemical Engineering Journal 526 (2025) 170335

Contents lists available at ScienceDirect

Chemical Engineering Journal

journal homepage: www.elsevier.com/locate/cej

Steroid hormone micropollutant removal from membrane bioreactor effluents using single-walled carbon nanotube composite nanofiber membranes

Han-Ya Lin [a], Minh N. Nguyen [a], Andrea I. Schäfer [a,*]

[a] Institute for Advanced Membrane Technologies (IAMT), Karlsruhe Institute of Technology (KIT), Hermann-von-Helmholtz-Platz 1, 76344, Eggenstein-Leopoldshafen, Germany

ARTICLE INFO

Keywords:
Adsorption
Carbon-based nanoparticles
Organic matter interference
Electrospinning
Physico-chemical water treatment
Wastewater reuse

ABSTRACT

Waterborne micropollutants can persist in wastewater effluents even after advanced treatment processes, such as membrane bioreactors (MBRs), posing significant risks to aquatic organisms and human. The incorporation of ultrafiltration (UF) membranes with adsorbents, such as single-walled carbon nanotubes (SWCNTs), provides a low-energy barrier against micropollutants, but water matrices can compromise function. Removal of steroid hormone 17β-estradiol (E2) micropollutants in synthetic water and MBR effluent is investigated with SWCNT;–UF composites with different configurations of feed- and permeate-side adsorption. Feed-side deposition of SWCNTs at a loading of 2.1 g/cm^2 in nanofiber mats achieves 96 % removal of E2 from synthetic water, while permeate-side deposition yields a lower removal of 73 % due to uneven SWCNT distribution in the non-woven UF support. With feed-side adsorption, E2 removal is limited by hydraulic residence time (12–30 milliseconds) rather than SWCNT loading (0.5–5.3 g/m^2). The removal of E2 that is spiked into MBR effluent was significantly lower, at around 47 %. This can be attributed to the direct and/or indirect competition of other micropollutants and organic matter in the MBR effluent for the adsorption sites of SWCNTs. The removal of other micropollutants that were identified in the MBR effluents was low. These results highlight the strong interference of MBR effluent organic matter and potentially other micropollutants to steroid hormone adsorption by composite membranes, and suggest permeate-side deposition of adsorbents may be a strategy to partially mitigate this interference.

1. Introduction

Micropollutants, including pharmaceuticals, pesticides, industrial additives, steroid hormones, and *per*- and polyfluoroalkyl substances (PFAS), have been detected in domestic, agricultural, hospital, and industrial wastewater. These contaminants pose significant risks to aquatic organisms through bioaccumulation which induces deformities and reduces their activity, even when present at trace concentrations ranging from nanograms to micrograms per litre [1,2]. Among all micropollutants, steroid hormone micropollutants are naturally produced from human and livestock excretion [3] or synthetic sources, such as contraceptive pills [4]. Steroid hormone micropollutants are the most common endocrine-disrupting chemicals. They interfere with the human endocrine system at even trace concentrations, increasing the risk of prostate, lung, endometrial, and breast cancers [5–7]. Estrone (E1), 17β-estradiol (E2), and 17α-ethynylestradiol (EE2) are compounds that warrant global attention [8]. In 2011, the European Commission proposed limiting E2 and EE2 concentrations in surface water to 0.4 and 0.04 ng/L, respectively, due to their potential hazards to aquatic life [9]. However, this was not enacted into European Union legislation, while a recent proposal suggests even lower concentrations of 0.18 and 0.02 ng/L [10]. To comply with these guidelines and prevent steroid hormone micropollutants from entering surface water, which often serves as a downstream drinking water intake, additional treatment processes are required.

In wastewater treatment plants (WWTPs), membrane bioreactors (MBRs) combine activated sludge with membrane filtration [11], demonstrating advantages such as high water recovery, greater effluent quality, and a smaller bioreactor size compared to the conventional activated sludge process [11,12]. Although high removal of steroid hormone micropollutants has been reported, removal depends on various factors, including operating parameters, physicochemical

* Corresponding author.
E-mail address: andrea.iris.schaefer@kit.edu (A.I. Schäfer).

https://doi.org/10.1016/j.cej.2025.170335
Received 16 June 2025; Received in revised form 27 October 2025; Accepted 29 October 2025
Available online 31 October 2025

properties of micropollutants, and influent quality [12–15]. To enhance effluent quality, several MBR operating parameters, such as sludge retention time, hydraulic retention time (HRT), pH, and temperature are adjusted [13,14]. The physicochemical properties of steroid hormone micropollutants also play a role. Hydrophilic micropollutants with electron-withdrawing groups (e.g., chlorine and amide) groups, are usually resistant to biodegradation (< 20 %), whereas micropollutants with electron-donating groups exhibit high removal (> 70 %) [12,15]. Seasonal variations can further impact partial removal of micropollutants; for instance, E2 and testosterone (T) were detected in MBR effluent at concentrations of 4 and 17 ng/L, respectively [16]. Incomplete removal of 85–93 % was also reported by Guo et al., with E1 and EE2 present in MBR effluent at concentrations of 81–251 ng/L and 174 ng/L, respectively [17]. Conventional and biological wastewater treatment processes (e.g., activated sludge and MBR) as well as advanced treatments (e.g., UV, ozone, and chlorine dioxide ClO_2), have been reported to be ineffective at removing steroid hormone micropollutants [18,19]. Therefore, additional treatment is required to ensure compliance with the European surface water guidelines.

Regarding micropollutants in WWTP effluent, in 2022, the European Commission proposed implementing 'quaternary treatment' as a mandatory infrastructure upgrade [20]. This stage, implemented after tertiary treatment (e.g., MBR processes), aims to remove emerging contaminants [21]. Filtration technologies used in WWTPs, such as nanofiltration and reverse osmosis, remove micropollutants through size exclusion [22–24], but these processes require high energy input to generate the required pressure for permeation [25]. Furthermore, steroid hormone micropollutants can be adsorbed and pass through the membrane, which requires further treatment [26,27]. Ozonation has been demonstrated as an effective tertiary treatment process in WWTPs [28–31]. Moreover, this technology has also been implemented in the WWTPs in the German states of North Rhine-Westphalia and Baden-Württemberg [32]. Emerging advanced oxidation technologies with membranes, such as photocatalytic membrane reactors [33–37], and electrochemical membrane reactors [38–40], break down the chemical structure of steroid hormone micropollutants through reactive oxygen species or direct electron transfer. However, the disadvantage of using these advanced oxidation technologies is the potential generation of oxidation by-products of micropollutants, which require additional treatment, such as downstream adsorption [41].

To address the presence of micropollutants in the effluent from tertiary wastewater treatment, adsorption is a well-established option. This technology is favoured in WWTPs due to its operational simplicity, high selectivity of adsorbents, and ease of regeneration [42]. Among adsorbents, activated carbon is widely used in WWTPs, typically in two forms: granular activated carbon (GAC), with particle sizes in the millimeter range, and powdered activated carbon (PAC), with particle sizes in the mid-micrometer range. GAC is generally applied in fixed-bed reactors, whereas PAC is used in slurry systems [42]. For example, at the Neugut WWTP in Dübendorf, Switzerland, GAC has been implemented downstream of ozonation. This configuration has demonstrated effective removal of biodegradable ozonation transformation products, oxidation by-products, and other micropollutants, maintaining efficiency for up to 500,000 bed volumes—equivalent to approximately two years of operation [30]. The 'ozonation + GAC' combination has also been applied in German WWTPs [32,43]. Alternatively, PAC is often applied as a post-treatment step following the activated sludge process to enhance micropollutant removal [31,32,44,45].

Regarding steroid hormone micropollutants, GAC and PAC achieved 90 and 98 % removal of E1 and estradiol valerate, respectively [46,47]. Polymer-based spherical activated carbon (PBSAC) – which is GAC produced via controlled synthesis – offers uniform sizes and pore distribution and has demonstrated good steroid hormone micropollutant removal (86–99 %) when packed in a thin layer (with thicknesses between 1 and 6 mm) [48]. A similar (60–90 %) removal of steroid hormones was achieved even in the presence of organic matter (humic acids and natural organic matter), suggesting that the organic matter might not enter the pores of PBSAC to interfere with steroid hormone adsorption [49]. Novel carbon-based materials [46–48] are characterized by a high specific surface area and strong hydrophobicity, and they do not release toxic by-products during quaternary treatment. Novel nanomaterials, such as carbon-based nanoparticles and some bottom-up designed advanced structures, are under various stages of development in the laboratory. Many of these materials are facing critical challenges for scale-up and real-life application [50,51].

Various carbon-based nanoparticles had been investigated in previous work for the removal efficiency of steroid hormone micropollutants, including graphene, graphene oxide, multi-walled carbon nanotubes (MWCNTs), single-walled carbon nanotubes (SWCNTs) and fullerene [52]. SWCNTs showed very high adsorption capacity and superior adsorption kinetics because the micropollutants can easily find the adsorption sites on the external surface of adsorbents [52]. SWCNTs possess a high specific surface area (200–800 m^2/g) [52–54] with half of their surface being external surface. Within a short HRT of less than a minute (sub-seconds to seconds), typical in membranes [55], the high external surface allows rapid adsorption of micropollutants. As a result, SWCNTs can be integrated with membranes [56,57] or prepared as buckypapers [58] to remove micropollutants in continuous flow. However, organic matter in the water matrices can interfere strongly with micropollutant adsorption at the external surface of SWCNTs [56]. This can be alleviated by the deposition of adsorbent materials on the permeate-side (i.e., into the support structures) where the ultrafiltration (UF) membrane can shield the effect of organic matter on micropollutant adsorption [56].

When nanomaterials are used, concerns exist regarding SWCNT toxicity once leached into the environment [59–61]. At concentrations of a few micrograms per litre, SWCNTs can inhibit the metabolism and neuroactivity of aquatic organisms [62–65]. Although there are currently no regulatory concentration limits for SW-/MWCNTs by the US Environmental Protection Agency, the European Union, or the World Health Organization, the concentrations of SW-/MWCNTs in surface water and even wastewater effluent are expected to be low. The predicted concentrations of carbon nanotubes in surface water and wastewater effluent are 0.001–0.004 and 8.6–14.8 ng/L [66,67]. Because the predicted toxicity thresholds are high (sub-milligram- to milligram-per-litre concentrations) and SW-/MWCNTs tend to undergo passivating transformations in the environment, the overall ecological risk is considered low [51]. However, concerns still arise because the SW-/MWCNTs in water are not quantifiable or even detectable owing to the large distribution of lengths, conformations, aggregation states, and varying capability to partition to colloids and organic matter [68,69]. As the valid concerns remain, it is highly unlikely that SW-/MWCNTs will be used in potable water treatment. SW-/MWCNTs are restricted to fundamental research and model adsorbents for various composite membranes, as long as research findings are transferable to materials that are more suitable or more ready for industrial application. These materials, including PAC, GAC, and other advanced nanoporous materials such as PBSAC, can be generated at a large scale and are much less prone to leakage due to the larger sizes.

In fundamental research, several methods have been explored to immobilize carbon-based nanoparticles in membrane materials. These include coating [70], solution blending [71], vacuum infiltration on the surface of UF membranes [72,73] (Fig. 1 A), loading nanoparticles inside microfiltration membranes pores [74,75] (Fig. 1 B), incorporating nanoparticles during fabrication [76] (Fig. 1 C), loading nanoparticles onto nanofiber layers [70,77] (Fig. 1 D), and vacuum infiltration in the non-woven support of UF membranes (Fig. 1 E) [56]. Among these methods, vacuum filtration [77] introduces minimal alterations to the surface properties of carbon nanoparticles, making it particularly suitable for application within membrane pore spaces [56]. When being deposited in the support structures (on the permeate-side, see Fig. 1 E), the SWCNT distributes unevenly due to aggregation, and as a result,

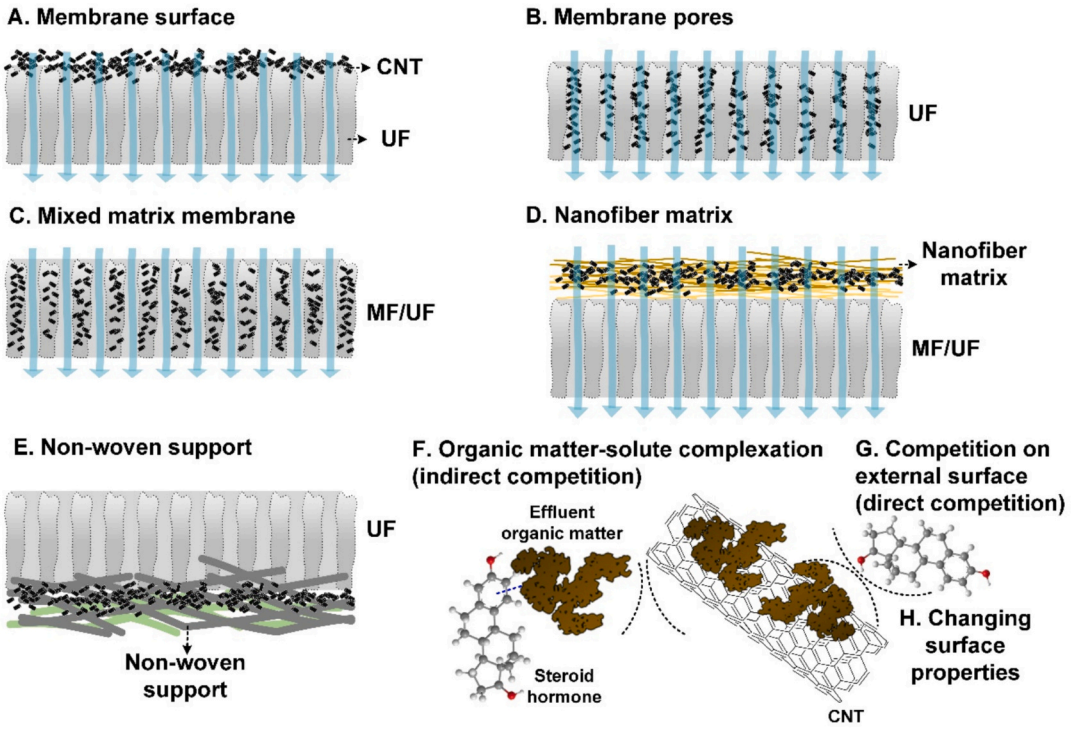

Fig. 1. Schematic of (A–F) incorporation of SW-/MWCNTs into membranes and (G, H) interference mechanisms of organic matter and steroid hormone adsorption on single-walled carbon nanotubes.

micropollutants in solution may transport dominantly through paths with the lowest SWCNT densities [78]. On the feed-side, infiltrating SWCNTs into the nanofiber matrix of composite membranes (Fig. 1 D) provides space for SWCNT loading while the support membrane prevents nanoparticle leakage [79]. However, organic matter interference is potentially stronger compared to permeate-side deposition, in which case the membrane may remove a significant amount of organic matter.

Effluent organic matter from wastewater treatment plants contains soluble microbial products (due to incomplete degradation of polysaccharides and proteins from cell lysis), humic substances and low-molecular-weight acids generated during biological processes [80–82], while in MBR effluent, the effluent organic matter is composed of high-molecular weight biopolymers, high proportion of humic substances, building blocks and low-molecular-weight acids, as characterized by liquid chromatography – organic carbon detection (LC–OCD) [83–85]. These organic substances can interfere with micropollutant adsorption by competing for adsorption sites on SW-/MWCNTs, blocking active sites/pores, altering surface properties, and inducing micropollutant−organic matter interactions [56,86–88]. The two main interference mechanisms are illustrated in Fig. 1 F and G). To minimize the negative impacts of MBR effluent organic matter on micropollutant adsorption, adsorbents can be deposited on permeate-side of the UF membrane (Fig. 1 E). With the permeate-side deposition, membranes with a molecular weight cut-off (MWCO) of 3−10 kDa can effectively screen out biopolymers and humic substances [89], but not the low-molecular-weight compounds [90]. Such pretreatment will hence only partially improve the steroid hormone adsorption capability of SWCNTs [56]. Conversely, feed-side deposition of SWCNTs in nanofiber voids or on UF membranes introduces potential interference from various contaminants, including natural organic matter surrogates such as humic acid [88,91] and fulvic acid [92]. These surrogates do not fully represent the composition of effluent organic matter that contains higher- and lower-molecular-weight fractions with varying interference potential.

Using electrospun nanofibers to immobilize SWCNTs on the feed side can serve as a microporous substrate (with few micrometer pores) for firm incorporation of SWCNTs and enhance the surface-to-volume ratio for SWCNT loading, potentially improving the removal of steroid hormone micropollutants at the expense of increased fouling potential. Permeate-side deposition may be able to remove some of the interfering organic matter, depending on the membrane used. Given that an additional membrane is required to avoid SWCNT leaching, the overall flow resistance is doubled [56]. While the incorporation of SWCNTs with UF membranes can combine tertiary and quaternary treatments for retaining pathogens and removing micropollutants, the fouling propensity of such a material may be enhanced. A comparison of recent studies using SW-/MWCNTs in adsorptive and reactive UF has been provided in Table S2.

This work will investigate the removal of steroid hormone micropollutants with permeate-side and feed-side SWCNT deposition in UF membranes and the interference of the MBR matrix on steroid hormone adsorption. The specific research questions are: (i) How much E2 adsorption is achieved when SWCNTs are incorporated in the permeate and feed sides of the UF membrane? (ii) What are the limiting factors—UF membrane properties, SWCNT loading, and HRT—that influence E2 removal from synthetic water using this method? (iii) To what extent does MBR effluent reduce E2 removal and uptake?

2. Materials and methods

2.1. Filtration system and protocol

The dead-end Perspex 10 mL stirred cell (Amicon 8010, Millipore, Germany) with a membrane of 2.5 cm diameter (effective membrane area of 3.8 cm^2), shown in Fig. 2, was used for membrane filtration experiments. The flux (Eq. S3) was controlled by the pump speed of a peristaltic pump (Masterflex L/S, Cole Parmer, Germany) equipped with 3 easy-load extensions (model 07516–10, Masterflex, Cole Parmer, Germany) and precision pump tubing (06442–14, Masterflex, Cole Parmer, Germany). A flux of 160 ± 60 $L/m^2{\cdot}h$ was selected as a standard condition and the filtration protocol is shown in Table S1. The raw data of filtration experiments are shown in Fig. S8 to Fig. S11.

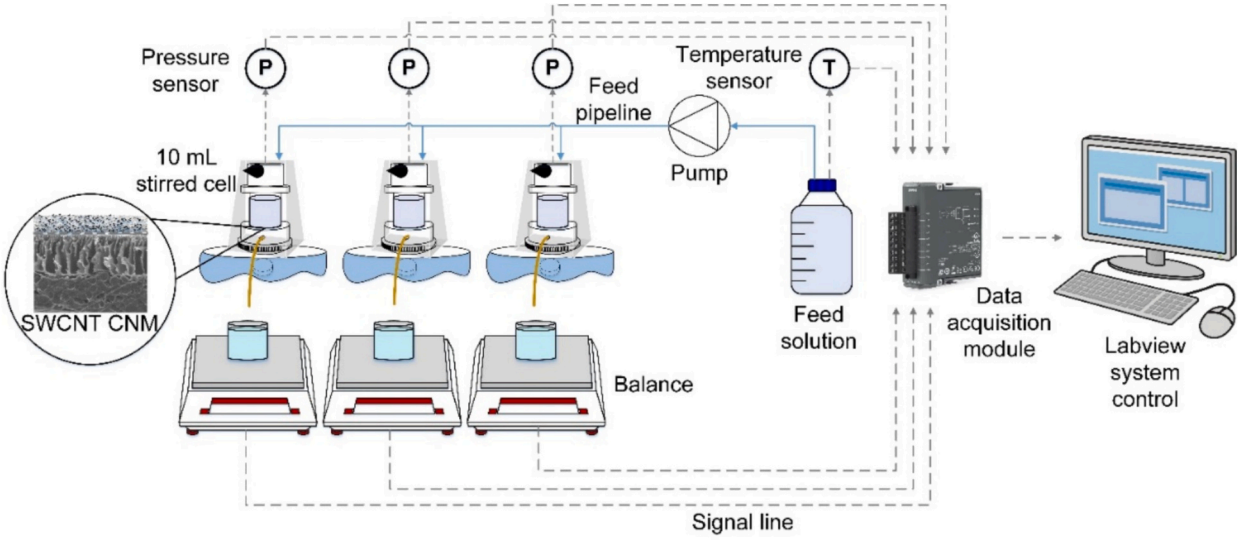

Fig. 2. Schematic of the Perspex 10 mL filtration system operated at constant flux.

2.2. Membrane and nanofiber materials

The polyethersulfone (PES) pristine membranes used as substrates were provided by ITÜ, Turkey, prepared using the non-solvent induced phase separation method [93]. The membrane codes with corresponding fabrication parameters and membrane properties are detailed in Table 1. It was anticipated that the membranes could be prepared with different support structures that hold variable SWCNT loadings. However, the support structures were not sufficiently open to enable a lot of nanoparticle infiltration (Fig. S1 A). Therefore, the feed-side deposition membranes were used for experimental investigation, while permeate-side deposition membranes at a relatively low SWCNT loading (2.1 g/m^2) were used for comparison.

For the permeate-side deposition membranes (SWCNT sandwich membranes), a membrane coupon (the support side facing upward) was inserted at the bottom of a loading gadget that was composed of a 25 mm diameter stainless-steel filter holder (Millipore, USA) and a stainless-steel tube (self-made). A SWCNT solution was prepared by sonicating 0.1 g/L SWCNT (Elicarb SW Low Residue, Thomas Swan, UK) and 0.1 wt % Triton X-100 (Sigma-Aldrich, USA), and then the solution of SWCNTs was poured into the loading gadget. The loading gadget was pressurised at 2 bar of synthetic air until all SWCNT solution was filtered. After the infiltration of SWCNTs, the membrane coupon was kept wet in a plastic petri dish and stored in a cool room at 4 °C. The same type of PES membrane was placed underneath to cover the support side of the SWCNT-UF composite membrane to produce a 'sandwich' [56]. This permeate-side membrane is schematically shown in Figure. S1A.

For the feed-side deposition membranes, nanofibers were electrospun onto the membrane substrates. To prepare the nanofibers, a 3 mL solution of 25 % (*w/v*) polyethersulfone (PES, 3000P, Solvay, Belgium) was prepared by dissolving PES powder in dimethylformamide (DMF, 99.8 %, Sigma-Aldrich, USA). The solution was stirred magnetically and heated on a hot plate (VMS—C7, VWR, Germany) at 50 °C for 12 h. Nanofibers were electrospun directly onto PES membranes using a high-voltage power supply (HPC-14-20000, FuG Elektronik GmbH, Germany) set to 17 kV, with a syringe pump (LA100, Landgraf Laborsystem HLL GmbH, Germany) operating at a controlled flow rate of 0.8 mL/h. The setup included a 19-gauge needle, a tip-to-collector distance of 15 cm, and a collector equipped with an x-y controller (SMC 200, MOVTEC Wacht GmbH, Germany) [95].

For the feed-side membranes (SWCNT composite nanofiber membranes), the composite nanofiber membrane was subjected to the same SWCNT infiltration process as the permeate-side deposition membranes. The feed-side membrane is shown in Fig. S1 B. A theoretical maximum SWCNT loading of 63 g/m^2 was estimated within the nanofiber matrix, which was electrospun using 3 mL of the electrospinning solution. The equations for calculating SWCNT loading are listed in Table S6. The electrospinning solutions (volumes of 0.75, 1.5, 3.0, 4.5, 6.0, 7.5 and 9.0 mL) were electrospun for the corresponding SWCNT loading (0.5, 1.0, 2.1, 3.1, 4.2, 5.3 and 6.3 g/m^2).

2.3. Membrane characterization

A scanning electron microscope (SEM, Supra 60VP, Zeiss, Germany) was used to visualize nanofiber morphology and cross-section. Membrane sample coupons were coated with a 15 nm gold layer using a sputter coating system (MED020, Bal-Tec, Germany). The software ImageJ (1.54d, USA) was used to analyze nanofiber diameter and

Table 1
Membrane code, fabrication parameters and properties [93]. Abbreviations: PES – polyethersulfone; PVP – polyvinylpyrrolidone.

No	Membrane code	Fabrication parameters			Membrane properties				
		Coagulation temperature (°C)	PES (%)	PVP (%)	Porosity[1]	Thickness (μm)	Average pore diameter[2] (nm)	Pore diameter in skin layer[3] (nm)	Permeability[4] (L/m^2.h.bar)
1	M1	25	20	8	0.66	90	40	2.9	131
2	M2	25	16	6	0.64	90	53	3.9	232
3	M3	50	16	6	0.73	90	85	4.3	314

[1] Calculated by Eq. S5.
[2] The average pore diameter was calculated by Eq. S7.
[3] Pore diameter was calculated by Eq. S7 assuming 0.5 μm as the skin layer thickness [94].
[4] Calculated by Eq. S4.

membrane thickness. To analyze the void size of the nanofiber matrix, SEM images were processed to black and white by ImageJ (v 1.54d), and 100 random voids were measured to calculate the average void size following a previously published procedure [96].

2.4. Solution chemistry and steroid hormone micropollutants

For experiments with synthetic water, a 100 mM NaCl (99.5 %, Thermo Scientific) and a 10 mM $NaHCO_3$ (100 %, VWR) stock solutions were prepared. Experiments were carried out in a background electrolyte of 10 mM NaCl and 1 mM $NaHCO_3$ (ten times dilution from the stock solutions) with a neutral pH of 8.1 ± 0.2. Ultrapure Milli-Q water (Milli-Q® Reference A+, Merck) was used for preparing stock hormone solutions, stock background electrolyte solutions, and feed water.

The radiolabeled [2,4,6,7-^{3}H] estrone (E1, 3.48 TBq/mM), [2, 4, 6, 7-3H] 17β-estradiol (E2, 2.59 TBq/mM), [1,2,6,7-^{3}H] progesterone (P, 3.63 TBq/mM), and [1,2,6,7-^{3}H] testosterone (T, 2.94 TBq/mM) (Perkin Elmer, USA) solutions were prepared by diluting a 10 μg/L stock solution to a final concentration of 100 ng/L with a background solution containing 10 mM NaCl and 1 mM $NaHCO_3$. Similarly, the MBR effluent with radiolabeled E2 was prepared by spiking MBR effluent with the 10 μg/L E2 stock solution to a concentration of 100 ng/L. E2 was selected as the specific target of removal because (i) E2 has been widely detected in MBR effluent [16], (ii) E2 has high toxicity to aquatic life and humans [97,98], and (iii) E2 was suggested in the watch list by the European Commission in 2022 [99]. The E2 concentration of 100 ng/L is adopted as a representative feed concentration in this study because similarly high concentrations in WWTP effluents have been reported [100–102].

2.5. Membrane bioreactor effluents

The MBR effluent samples were obtained from Japan (Soseigawa Wastewater Treatment Center, Sapporo), Turkey (Ağva Advanced Biological WWTP, Istanbul), Germany (Nordkanal WWTP, Rhine-Westphalia) and France (Pont-du-Casse WWTP, Pont-du-Casse). The process design differs for these plants as well as the effluent organic matter and the primary purpose was to evaluate the interference with steroid hormone adsorption. After transport, all MBR effluent samples were stored in a cool room at 4 °C to reduce the growth of bacteria prior to experiment. The analyzed micropollutant concentrations, effluent characteristics and flow diagrams of MBR WWTPs are detailed in Fig. 9, Table S4 and Fig. 7 (right), respectively.

The Japanese effluent sample was collected in July 2023 from the Soseigawa Wastewater Treatment Center, which processes 140,000 m^3/day of municipal wastewater. The designed baffled MBR consists of two compartments (aerobic and anoxic zones) and a membrane unit installed on one side of the compartments. The membrane element contains hollow-fiber membranes made of polytetrafluoroethylene with a pore diameter of 0.2 μm. The reported biochemical oxygen demand removal exceeds 98 % [103]. The baffled MBR was reported to have better nitrogen and phosphorus removal compared to conventional submerged MBR [104]. However, a higher concentration of nitrate was analyzed from the effluent shown in Table S4, suggesting incomplete nitrogen removal in denitrification (anoxic), as it is the limiting step for nitrogen removal in the baffled MBR [104,105].

The German effluent sample was collected in November 2023 from the Nordkanal WWTP, which treats municipal wastewater from Kaarst and is designed for 80,000 population equivalents, equating to 16,000 m^3/day. The influent of Nordkanal WWTP passes through a coarse screen; ferric chloride is added to the water to enhance coagulation. Then, sand and grit particles are separated from the sand removal process. The membrane element comprises hollow-fiber membranes made of polyvinylidene difluoride (PVDF) with a pore diameter of 0.04 μm. The documented biochemical oxygen demand removal is approximately 98 % [106].

The French effluent sample was collected in March 2024 from the Pont-du-Casse WWTP, which treats municipal and industrial wastewater from Pont-du-Casse, handling 1857 m^3/day. The membrane element contains hollow-fiber membranes made of PVDF with a pore diameter of 0.015 μm [107,108].

The Turkish effluent sample was collected in October 2023 from the Ağva Advanced Biological WWTP, which treats 8000 m^3/day of municipal wastewater. The influent of Ağva MBR advanced biological WWTP passes through a series of sand removal stages with decreasing particle sizes (20 μm, 6 μm and 1 μm) [109]. The membrane element comprises hollow-fiber membranes made of PVDF with a pore diameter of 0.04 μm [110,111].

2.6. Water quality analysis

A liquid scintillation counter (LSC, Tri-Carb 4910 TR, PerkinElmer, Germany) was used to determine the concentration of radiolabeled steroid hormones and calculate the steroid hormone removal. LSC calibration was performed by measuring the activity of tritium (Bq) in samples of known steroid hormone standard concentrations (0, 0.05, 0.1, 0.4, 1, 10, 50 and 100 ng/L) which were prepared by dilution of the steroid hormone stock solution. The LSC calibration curve is shown in Fig. S5 and equations for calculating steroid hormone removal (Eq. S1) and mass adsorbed (Eq. S2) are detailed in Table S3.

A pH/conductivity meter (pH/Cond 3320, WTW, USA) with a pH sensor (SenTix® 41) was used for pH and conductivity measurement.

A total organic carbon (TOC) analyzer (TOC-L, Shimadzu, Japan) with non-purgeable organic carbon mode was used to determine TOC in MBR effluents. A UV − Vis spectrometer (Lambda 25, Perkin Elmer, USA) with rectangular cuvettes (10 mm path length, 3.5 mL, Agilent, USA) was used to measure the absorbance of organic matter in the wavelength range of 200–700 nm. The specific UV absorbance ($SUVA_{254}$) was calculated by dividing the UV absorbance at 254 nm by the TOC value [112]. The calibration of TOC is shown in Fig. S6.

A liquid chromatography – organic carbon detection (LC − OCD, Model 9, DOC-Labor, Germany) was employed to quantify the fractions of organic matter components. Liquid chromatography-organic carbon detector (LC–OCD) categorizes the dissolved organic carbon into five fractions, which are biopolymers (e.g., polysaccharides and proteins, molecular weight (MW) > 20,000 Da); humic substances (MW 500–1000 Da); building blocks (breakdown products of humic substances, MW 300–500); low molecular weight neutrals (mono-oligosaccharides, alcohols, aldehydes and ketones, MW < 350 Da); and low molecular weight acids (monoprotic organic acids, MW < 350 Da) [113].

An ion chromatography instrument (IC, Metrohm 580 Professional, Metrohm, Switzerland) with an anion exchange column (Metrosep A Supp 5, Metrohm) and a cation exchange column with a guard column (Metrosep C 4–150/4.0, Metrohm) enabled the determination of anion and cation concentrations in MBR effluents and permeate solutions. Metals/trace inorganics (Al, As, Ba, Be, Co, Cr, Cu, B, Sr, Fe, Mn, Mo, Ni, Se, and U) were analyzed by an inductively coupled plasma mass spectrometry (ICP-MS) (model J8403A 7900 Agilent, Japan). The calibration curves of different elements are summarized in Fig. S7.

Micropollutant screening for MBR effluents and permeate solutions was analyzed by Technologiezentrum Wasser (TZW, Karlsruhe), following standard protocols identity of the micropollutants for analysis, standard protocols, and limit of quantification (LOQ) are listed in Table S5.

3. Results and discussion

To confirm that the SWCNT can be loaded into the permeate-side and feed-side deposition membranes, the surface and the cross-section of the membranes will be visualized by SEM. Then, following the comparison of steroid hormone removal with the two set-ups, several filtration factors will be investigated with the feed-side deposition, including UF

membrane properties, SWCNT loading, and HRT. Finally, different MBR effluents will be spiked with radiolabeled E2 to elucidate the interference of MBR effluent organic matter on E2 removal.

3.1. Evaluation of the SWCNT loading in permeate-side and feed-side deposition

To assess SWCNT accessibility within the non-woven support of permeate-side deposition and the nanofiber matrix of feed-side deposition, surface and cross-section morphologies were examined using SEM. Fig. 3 A, E illustrates differences in membrane surface composition. The feed-side deposition consists of overlapping nanofibers, while the permeate-side deposition is composed of tightly packed melted polymer and non-woven fabrics, which exhibit low porosity, consistent with literature using commercial non-woven fabrics [78,114,115]. The nanofiber matrix contains more voids, which are advantageous for SWCNT loading. In contrast, SWCNTs cannot be effectively loaded into the non-woven fabric due to restricted void access. Nevertheless, both membrane surfaces are covered with SWCNTs, as shown in Fig. 3 B, F.

Fig. 3 F, G shows the presence of SWCNTs on the nanofiber surface and within the cross-section of the feed-side deposition. The nanofiber matrix, with a thickness of 36 ± 1 μm, was successfully loaded with 2.1 g/m^2 SWCNTs. The cross-sectional SEM image in Fig. 3 H confirms SWCNT integration within the nanofiber matrix of the feed-side deposition. In contrast, two clear layers can be observed in permeate-side deposition (Fig. 3 C), the SWNCTs layer on top and the non-woven support on the bottom. Nonetheless, the zoom-in image in Fig. 3 D shows the absence of SWCNTs in the cross-section of the permeate-side deposition, indicating that SWCNTs are primarily restricted to the surface of the non-woven support.

The Brunauer-Emmett-Teller specific surface area of free SWCNTs has been reported in the previous research (775 m^2/g), the zeta potential of SWCNTs was reported to be neutral or slightly negative at all pH, and the X-ray photoelectron spectroscopy of the SWCNTs showed 98.1 % carbon on their surface and 1.9 % oxygen, indicating its hydrophobicity while most of the carbon was in sp^2 configuration (90.7 %), forming aromatic structure [52]. Because the incorporation of SWCNTs in the membrane is purely physical and does not involve chemical alterations, the physiochemical structure of incorporated SWCNTs may not vary from that of free SWCNTs. It is possible that the aggregation state of SWCNTs limited the access of micropollutants to the SWCNT surfaces, especially within the short HRT in membrane filtration. Additionally, some SWCNTs can leak through the UF membrane, although the estimated pore diameter of the selected UF membranes is 4.3 nm and can retain the SWCNT principally (2–3 nm of diameter and 1 μm of length, although the aggregates are much larger) [78].

The SEM images confirm that SWCNTs were successfully loaded into the nanofiber matrix of the feed-side deposition. The next step is to assess whether the nanofiber matrix enhances E2 removal. Membranes with both permeate-side and feed-side SWCNT deposition will be evaluated for steroid hormone removal.

3.2. Adsorption of estradiol using varied membrane configurations

To compare the E2 removal of the two membrane depositions, SWCNTs were incorporated at a loading of 2.1 g/m^2. Additionally, experiments were conducted using membrane filtration with an E2 concentration of 100 ng/L and a flux of 160 L/m^2.h. The breakthrough curves, E2 removal, and mass adsorbed are presented in Fig. 4.

The breakthrough curves in Fig. 4 A, B show that pristine PES membranes (M1, M2, and M3) gradually approached the feed concentration, suggesting that adsorption was nearing saturation. In contrast, permeate-side deposition (P-M1, P-M2, and P-M3) reached equilibrium after collecting 150 mL of permeate, while feed-side deposition (F-M1, F-M2, and F-M3) exhibited an extremely low concentration profile. The permeate-side and feed-side depositions demonstrated a higher E2 removal than the PES pristine membranes, which achieved only 5 to 20 % removal. This improvement was attributed to the loaded SWCNTs, which provided abundant active sites for adsorption. The specific surface area of SWCNTs (775 m^2/g) is significantly higher than the 4 to 20 m^2/g reported for self-fabricated and commercial PES/polysulfone UF membranes [116–118].

Feed-side deposition achieved 96 % E2 removal, outperforming permeate-side deposition, which showed removal of 50 to 80 %. Similarly, 60 to 80 % E2 removal was reported from permeate-side deposition using commercial PES UF membranes [78], indicating the reproducibility of performance with SWCNT composite membranes. The higher E2 removal can be explained by the better accessibility of SWCNTs within the nanofiber matrix when deposited on the feed-side, as seen in Fig. 3 D. These findings confirm that feed-side deposition enhances E2 adsorption due to the improved distribution of SWCNTs in the nanofiber matrix. The removal of other steroid hormones (E1, T, and P) by feed-side deposition was high and vary between 50 and 80 %, following the order E2 > P > T > E1 (Fig. S4).

The results of E2 removal demonstrated feed-side deposition enhances E2 adsorption owing to the better distribution of SWCNT in the nanofiber matrix. In the next section, the SWCNT loading will be varied to examine the impact on membrane permeability and whether the permeate concentration can be further reduced to meet the European Union guideline.

3.3. Estradiol removal and membrane permeability with SWCNT loading

Loading SWCNTs into the nanofiber matrix of feed-side deposition

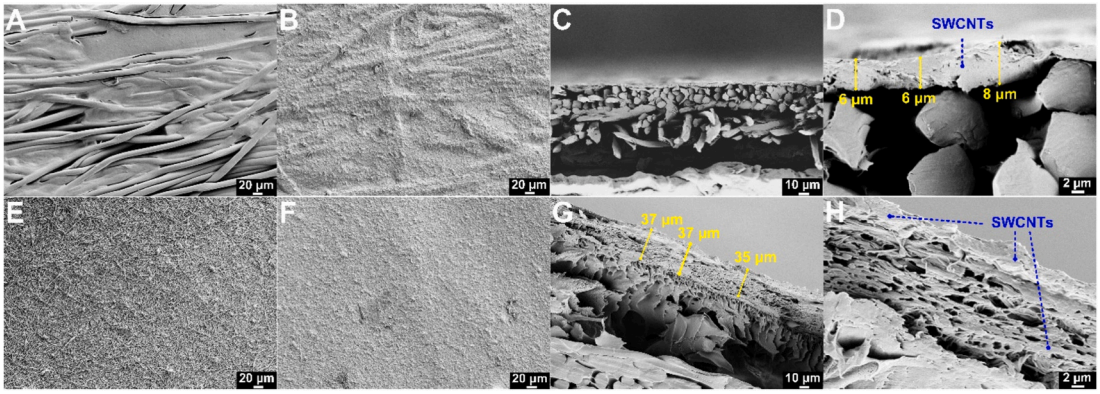

Fig. 3. SEM images of (A) surface of permeate-side deposition (M1) without SWCNTs, (B) surface of permeate-side deposition loaded with SWCNT, (C) cross-section of permeate-side deposition loaded with SWCNTs, (D) zoom-in of M1, (E) surface of feed-side deposition (F-M1) without SWCNTs, (F) surface of feed-side deposition loaded with SWCNT, (G) cross-section of feed-side deposition loaded with SWCNTs and (H) zoom-in of F-M1.

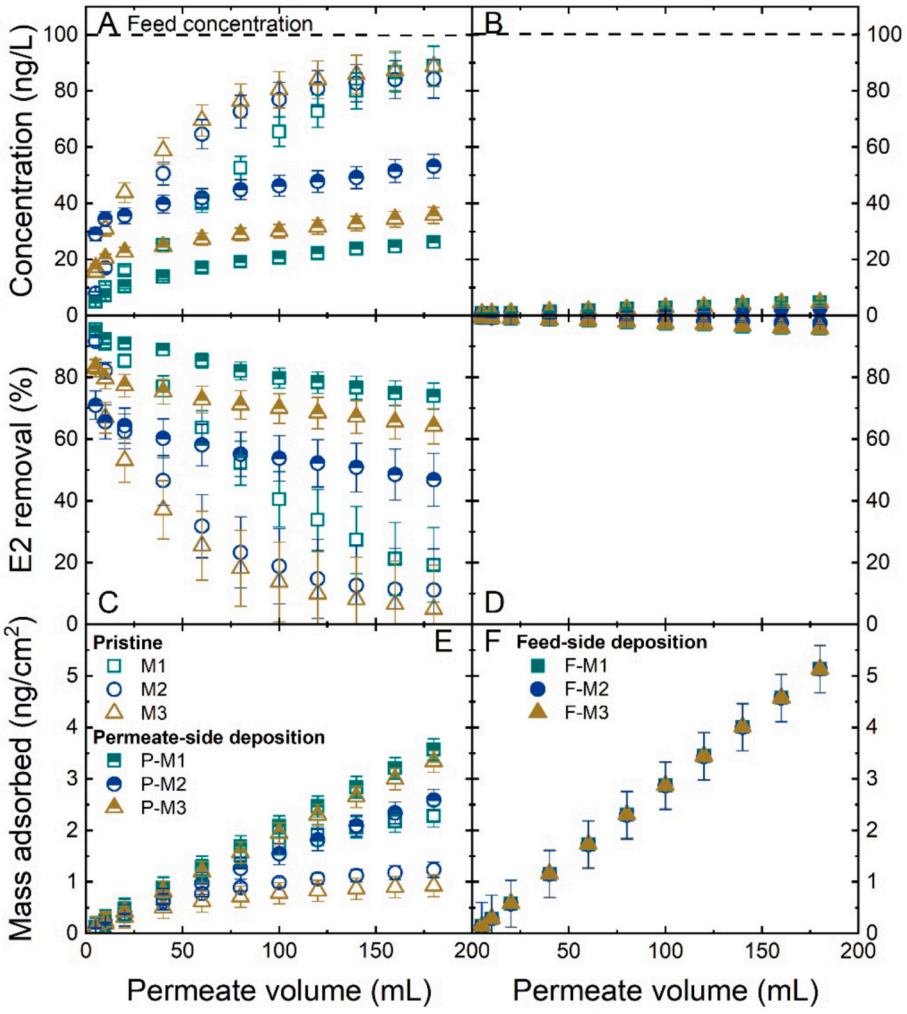

Fig. 4. (A, B) Permeate concentration, (C, D) E2 removal and (E, F) mass adsorbed as functions of permeate volume with various membrane configurations. SWCNT: 2.1 g/m^2 for permeate-side and feed-side deposition, 160 ± 16 L/m^2.h, 1 mM $NaHCO_3$, 10 mM NaCl, 22.5 ± 1, pH 8.1 ± 0.2.

may decrease permeability due to an increased resistance to water flow when some voids in the nanofibers are occupied by aggregated SWCNTs. Membrane resistance was calculated by Eq. S8; pure water permeability experiments were conducted for pristine membranes (M1), feed-side deposition (F-M1), and membranes with varied SWCNT loading (Fig. 5 C). To determine the optimal SWCNT loading for effective E2 removal, filtration experiments were performed with an E2 concentration of 100 ng/L, 160 L/m^2.h, and SWCNT loading ranging from 0.5 to 5.2 g/cm^2. The pure water permeability, membrane resistance, breakthrough curves, E2 removal, and mass adsorbed of different SWCNT loadings are shown in Fig. 5.

The pristine membrane (M1) exhibited a pure water permeability of ~200 L/m^2.h.bar and a corresponding membrane resistance of $2 \bullet 10^{12}$ m^{-1}, similar to that of the feed-side deposition without SWCNT loading (Fig. 5 B, C). This indicates that the nanofiber matrix does not significantly increase resistance. Dobosz et al. attached the nanofiber matrix to the UF membrane (25 μm thick), without applying heat treatment or adhesives, and determined that the pure water permeability was similar to that of the pristine membrane [79].

Feed-side deposition (F-M1) with varied SWCNT loadings exhibited membrane resistance values comparable to M1, suggesting that the major source of resistance comes from the base membrane M1. Further SWCNT deposition did not result in a significant increase in membrane resistance, likely due to the interconnected nanofiber matrix structure, which has relatively large void sizes of 1 μm (Fig. S2), compared to the skin layer pore diameter (3–4 nm) (Table 1), allowing efficient water flow.

In Fig. 5 B, the E2 removal increased from 85 to 96 % as SWCNT loading increased from 0.5 to 2.1 g/m^2. A higher loading did not improve the E2 removal. Although SWCNT aggregation can reduce the effective surface area available for adsorption [119,120], the low concentration of E2 results in several-order-of-magnitude lower total cross-sectional area of E2 molecules compared with the SWCNT surface area, suggesting that the SWCNT surface area may not be a limiting factor. However, SWCNT aggregates may become trapped on the nanofiber matrix, and higher SWCNT loadings may progressively block the nanofiber layer and prevent further SWCNT deposition in the depth of the layer. The denser the aggregates, the higher proportion of SWCNT surface not directly accessible to E2 within the short HRT. In other words, the diffusion of E2 molecules to the less accessible surfaces of SWCNT aggregates is a limiting factor [120]. However, when the loading was increased from 2.1 to 5.3 g/m^2, removal plateaued at approximately 96 to 98 %. In previously reported static adsorption studies, SWCNTs achieved 98 % E2 removal, which is the removal at the adsorption equilibrium, within 5 minutes [52]. It is implied that in this continuous-flow study, neither the SWNCT surface nor the mass transfer of E2 (from the bulk phase in the nanofiber 'pores' towards the most accessible surface of SWCNTs) are the limiting factors. Instead, adsorption was limited by the affinity between SWCNTs and the E2, which can be described with the adsorption equilibrium constant/

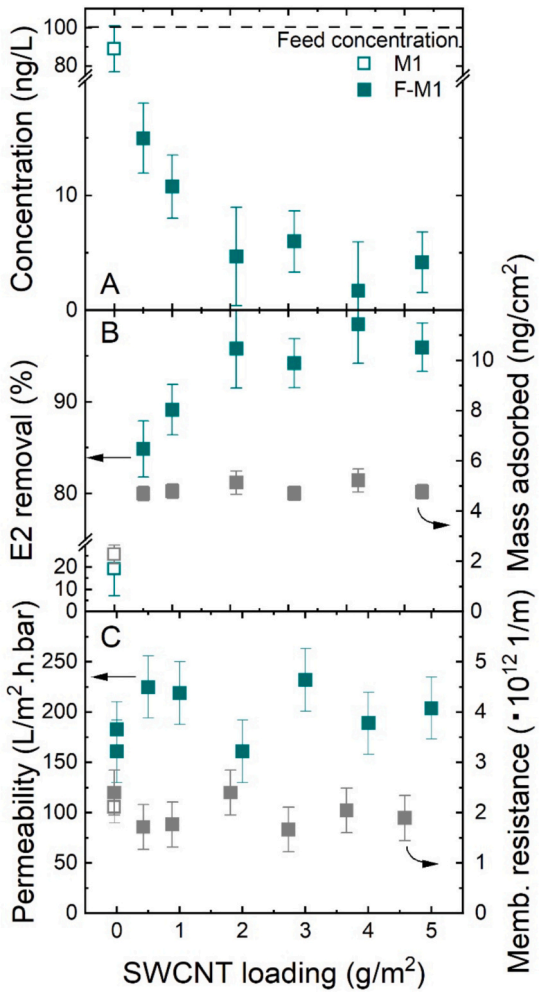

Fig. 5. (A) Permeate concentration, (B) E2 removal, mass adsorbed and (C) pure water permeability and membrane resistance as functions of SWCNT loading. F-M1, permeate volume 180 mL, 160 ± 16 L/m^2.h, 1 mM $NaHCO_3$, 10 mM NaCl, 22.5 ± 1 °C, pH 8.1 ± 0.2.

affinity constant in static adsorption [121,122]. Since increasing SWCNT loading did not result in a significant improvement in E2 removal, a loading value of 2.1 g/m^2 was selected as the standard loading for filtration experiments. To determine whether HRT is a limiting factor, membrane filtration experiments will be performed at various water fluxes.

3.4. Estradiol removal with varied hydraulic residence time

In micropollutant removal, mass transfer is a common limiting factor. Increasing HRT will enable overcoming mass transfer by allowing more time for E2 to diffuse onto SWCNT surfaces or into intra-pores of SWCNT aggregates. The pristine PES membrane (M3) was picked as the support for feed-side deposition (F-M3) due to its higher pure water permeability (Table 1). This ensures that transmembrane pressure remains below the filtration cell of 5.2 bar. To calculate the HRT, the thickness of the SWCNT nanofiber matrix (without the support membrane) was used in Eq. S6. The permeate concentration, E2 removal, and mass adsorbed at different flux are shown in Fig. 6. The permeate concentration reached 20 ng/L as the flux decreased from 1000 to 400 L/m^2.h, while E2 removal increased from 78 to 96 %. However, the mass adsorbed increased only by 1.3 times, from 3.9 to 5 ng/cm^2, as shown in Fig. 6 E, F, despite the higher mass flux of micropollutants.

The E2 removal increased with HRT from 3 to 12 milliseconds (corresponding to a flux decrease from 995 to 268 L/m^2.h), and then reached a plateau at 96 % removal at 12 milliseconds of HRT. From 12 milliseconds onwards (flux <268 L/m^2.h), HRT no longer limits adsorption, but instead, the affinity between SWCNT and E2 becomes the limiting factor. Below 12 milliseconds of HRT (flux >268 L/m^2.h), adsorption was limited by the transport of E2 from the bulk phase inside the pores to the adsorptive SWCNT surface. Although the total SWCNT surface is abundant, adsorption at high fluxes and low HRTs was limited by the mass transfer of E2 towards the accessible surface of the SWCNT aggregates.

Similar removal trends were reported using activated carbon fibers and SW-/MWCNTs [75,78,123], where steroid hormone micropollutants and organic dye removal plateaued at higher fluxes and transmembrane pressures. This phenomenon can be attributed to rapid adsorption kinetics, driven by the high surface area and surface properties that facilitate hydrophobic effect and π–π interactions with micropollutants [124]. Due to rapid adsorption kinetics, higher micropollutant removal can be achieved even with limited HRT. The feed-side deposition demonstrated high removal (78–96 %) in the lower flux range of 150–400 L/m^2.h.

In the next section, the effluents from wastewater treatment plants following the MBR step (containing various electrolytes, heavy metal ions, micropollutants, and organic matter) will be used instead of synthetic water to examine the E2 performance of SWCNT composite nanofiber membranes.

3.5. Estradiol removal with interference of MBR matrix using SWCNT composite membrane

To evaluate steroid hormone micropollutant removal in an MBR effluent matrix, and in particular the interference by other matrix compounds, filtration experiments were conducted using feed-side deposition (SWCNT loading: 2.1 g/m^2) at a flux of about 150 L/m^2.h. The MBR effluent was spiked with 100 ng/L radiolabeled E2 as the feed solution.

Fig. 7 represents the permeate concentration, E2 removal, and mass adsorbed, along with flow diagrams of each MBR wastewater treatment plant (WWTP) (Fig. 7, right). The breakthrough curves with different MBR effluents are shown in Fig. S3 J and the E2 removal is summarized in Table S7.

When MBR effluents were used as feed solutions, a significant reduction in E2 was observed, as shown in Fig. 7 B, where removal dropped from 96 to 50 %. In comparison with current treatment technologies, PAC, GAC, and ozonation have been evaluated in laboratory-scale batch adsorption or filtration experiments. Reported E2 removals exceed 92 % for PAC [125–127] and 80 % for GAC [128–130]. From literature, ozonation with high ozone doses (10 mg/L) has been shown to degrade E2 almost completely [131–133]. Higher performance was attained with synthetic water matrices, as such the composite nanofiber membranes are comparably effective (96−98% E2 removal). However, real water matrices impede the performance of various technologies. In WWTPs, a 61 % E2 removal was reported in two large-scale parallel pilot trials—one employing ozonation and the other using PAC followed by UF [31], while a full-scale GAC plant in a UK WWTP achieved an E2 reduction of over 50 % [134]. Similar reduction of E2 removal was observed in this work due to the water matrix. This indicates that real water interference studies, such as this work with SWCNTs as the model adsorbents, are important.

Fig. 7 (right), no significant differences were observed in E2 removal across the different MBR effluents, despite variations in pre-treatment methods, including baffled MBR, submerged MBR, and side-stream MBR. This suggests that the different water qualities in the four effluent samples did not significantly affect removal.

The specific mechanism (either direct competition for adsorption sites or indirect competition due to reduced affinity of E2−organic matter complexes for SWCNT surface) responsible for this reduction in

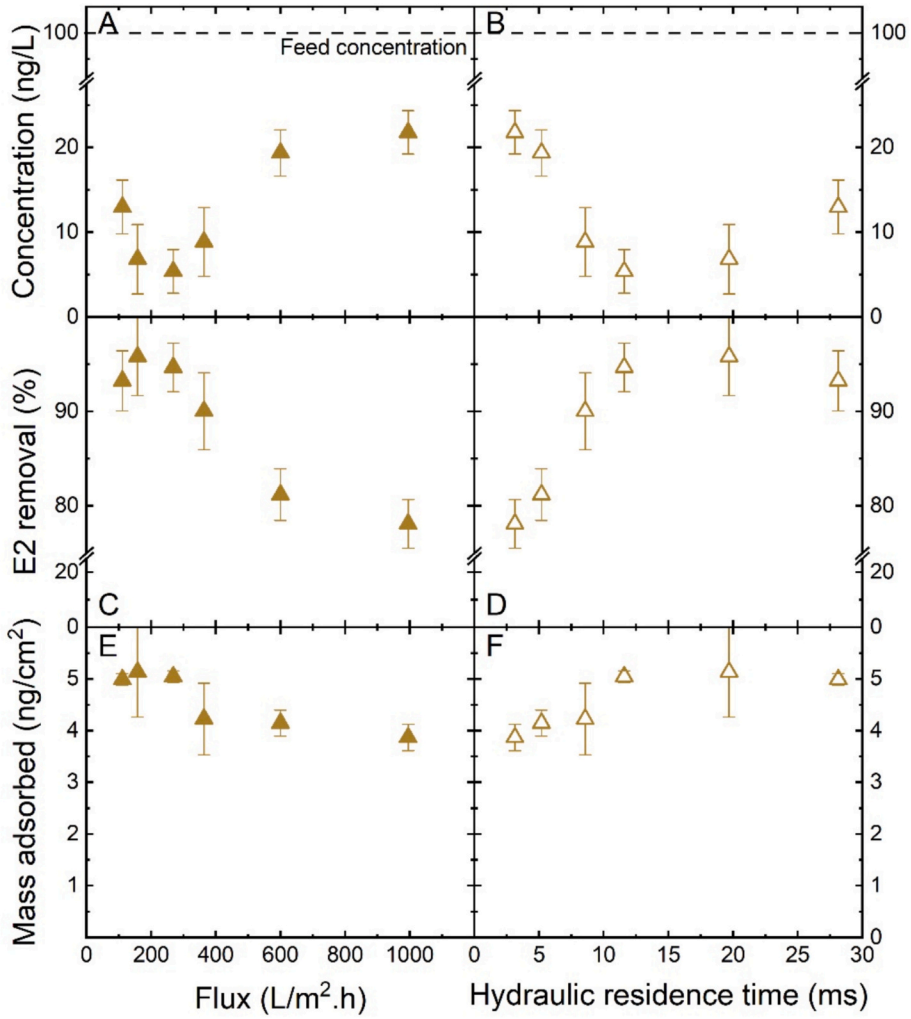

Fig. 6. (A, B) Permeate concentration, (C, D) E2 removal and (E, F) mass adsorbed as functions of flux and HRT. F-M3 (SWCNT: 2.1 g/m^2), permeate volume 180 mL, 1 mM $NaHCO_3$, 10 mM NaCl, 22.5 ± 1 °C, pH 8.1 ± 0.2.

E2 removal remains unclear. To further examine the possible mechanism of direct/indirect interference, water quality will first be analyzed by LC − OCD for organic matter fractions, followed by an assessment of micropollutant composition in the MBR effluents.

3.6. Examination of interference mechanisms from organic matter

To determine whether the reduction in E2 removal is due to competition for adsorption by effluent organic matter and other micropollutants, the raw MBR effluent, feed (spiked with 100 ng/L radiolabeled E2), and permeate samples after membrane filtration (permeate volume 180 mL) were analyzed by LC − OCD to compare the organic matter fraction. The TOC values of the MBR samples from Japan, Turkey, Germany and France are 3.9, 4.6, 4.6 and 6.2 mg/L, respectively. Other effluent characteristics are detailed in Table S4.

Among all MBR effluents, the Japanese effluent exhibited the highest UV signal, indicating a greater fraction of humic substances (Fig. 8). Additionally, the SUVA value for Japan MBR (3.1 L/mgC.m) is higher than that of other MBR effluents (1.9, 1.7, and 1.3 L/mgC.m for Turkey, Germany and France, respectively) shown in Table S4, suggesting a higher fraction of aromatic compounds. This can be attributed to the higher degradation of biopolymers in the Japan MBR, where biopolymers (aliphatic structures) degrade into humic substances that easily pass through the membrane [85,136]. The lower biopolymer fraction in the Japanese effluent, as shown in Fig. 8 A, further supports this finding.

In Table S4, significant reductions were observed in certain metal/inorganic concentrations, particularly Fe, Mn, Sr, and Zn, while other elements were minimally removed in post-membrane filtration. The reduction of Fe, Mn, Sr, and Zn can be attributed to adsorption by membrane materials [137], SWCNTs [138], and the formation of metal–organic matter complexes [139–141].

As shown in Fig. 8 C, D, a decrease in the low-molecular-weight acids fraction was observed in the permeate of German and French MBR effluents, but not in those of Japan and Turkey. This may be attributed to competition for adsorption sites by low-molecular-weight organic matter [142,143]. Wang et al. reported that low-molecular-weight hydroxyl and phenolic compounds compete for PAC adsorption sites, significantly reducing micropollutant removal from 86 to 90 % to 37–60 % [143]. Similarly, Zietzschmann et al. fractioned organic matter using UF, nanofiltration, and reverse osmosis to assess the impact of organic matter size on micropollutant removal by activated carbon, where findings demonstrated that the major reduction in removal is due to adsorption site competition by the smaller organic matter [142].

A slight decrease in the biopolymer fraction was observed in the permeate of Turkey and France, as shown in Fig. 8 B, D. However, the humic substance fraction, the dominant fraction of organic matter, remained unchanged when SWCNTs were deposited on the feed side. This suggests that major organic matter does not significantly compete for SWCNTs adsorption sites, although the order of magnitude difference in concentration may not enable detection in the appropriate

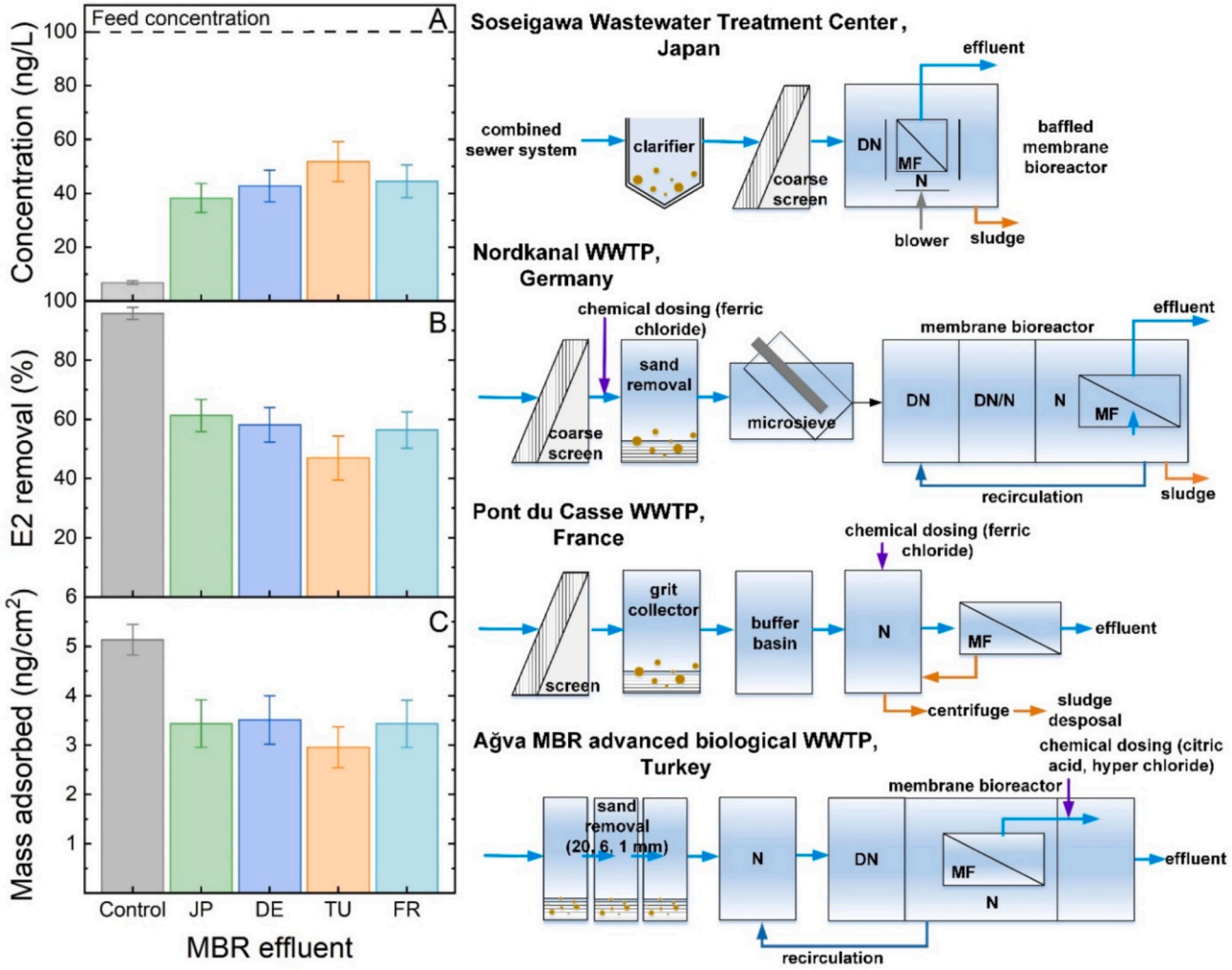

Fig. 7. (A) Permeate concentration, (B) E2 removal and (C) mass adsorbed as functions of Japan (JP), Germany (DE), Turkey (TU) and France (FR) effluents. F-M3 (SWCNT: 2.1 g/m^2), permeate volume 180 mL, 160 ± 16 L/m^2.h, 22.5 ± 1 °C. The 'control' experiment refers to the experiment conducted only with synthetic water (c_f 100 ng/L E2, 1 mM $NaHCO_3$, 10 mM NaCl). (Right) Flow diagrams of MBR plants.

range. Guillossou et al. reported that biopolymers and hydrophobic molecules cause pore blockage or form micropollutant–organic matter complexes that are progressively adsorbed at the PAC surface [135]. Neale and Schäfer found that steroid hormone micropollutants can partition into humic acid, and steroid hormone removal improved when humic acid concentration increased from 0 to 125 mgC/L using 10 and 100 kDa MWCO UF membranes [88]. Conversely, 10 kDa UF membranes have been shown to effectively screen organic matter and facilitate partial rejection of E2 that partitions into organic matter [56,88]. One major mechanism of interference in this study may be the formation of E2 – organic matter complexes, which is shown in Fig. 1 F, reducing the affinity of E2 for the SWCNT surface and hence results in lower E2 removal (indirect competition). The contact time between E2 and organic matter (at least 30 minutes, as these were mixed in the feed prior to the experiment) is significantly longer than the contact time between E2 and the SWCNT layer (20 milliseconds), supporting the indirect competition mechanism. Another mechanism is direct competition for adsorption sites, where organic matter adsorbs onto SWCNTs, thereby preventing E2 adsorption [142,143]. However, this mechanism is not strongly supported by the data, as SWCNT−UF exhibited negligible organic matter removal (see Fig. 8, OCD signals). As indicated above, this may be due to the insufficient instrument sensitivity for detecting organic matter adsorption. Pore blockage caused by organic matter could also hinder the micropollutant passage [135]. However, this mechanism is unlikely due to the small hydrodynamic diameter (0.8 nm) of E2 and the negligible removal of organic matter observed. Therefore, it appears advisable to incorporate adsorbents (SWCNTs) on the permeate side of UF membranes that are able to retain organic matter. While this approach has been shown to maintain good micropollutant adsorption performance, despite the presence of organic matter [56], low-molecular-weight fractions cannot be retained and may thus cause interference when MBR effluents that contain a very different organic matter composition are treated. Given the typically very low concentration of low-molecular-weight fractions, this is a challenging endeavour to examine.

Although other techniques have been used to characterize interactions between micropollutants and organic matter, such as fluorescence spectroscopy [144–147] and Fourier-transform infrared spectroscopy [148,149] via the shifts in and changes in intensity of characteristic peaks when organic matter binds to micropollutants. However, these techniques often require higher micropollutant concentrations than their occurrence in real waters for analysis and do not account for the synergistic effects of adsorbents (SWCNTs) in the system.

After analyzing the interference of major organic matter fractions on E2 adsorption, it is important to examine whether other micropollutants in MBR effluents directly interfere with E2 adsorption. To determine whether additional micropollutants in MBR effluents were removed and thus competed for adsorption sites, membrane filtration was performed,

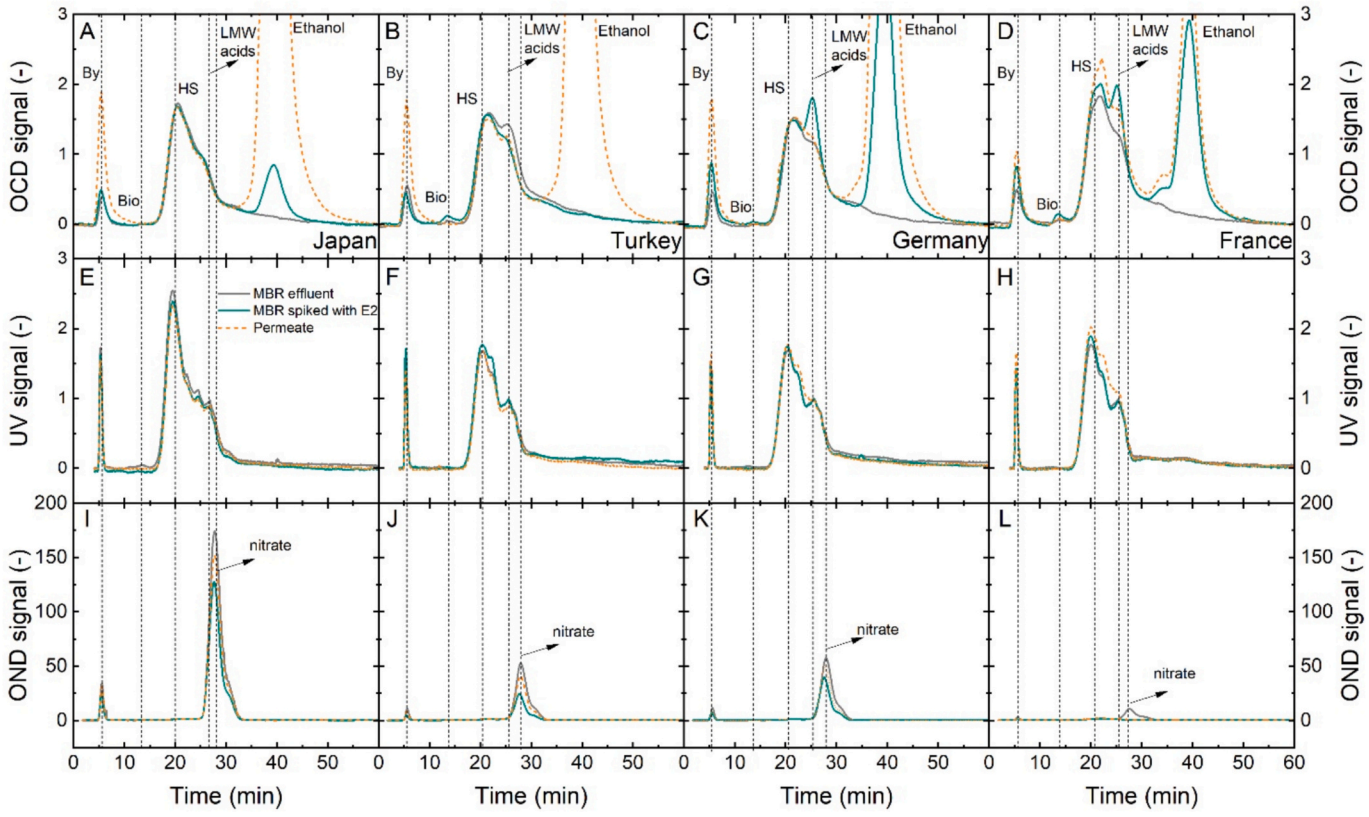

Fig. 8. Organic carbon (OCD) signal, UV signal and organic nitrogen (OND) signal of (A, E, I) Japan, (B, F, J) Turkey, (C, G, K) Germany and (D, H, L) France MBR effluents. Bypass: By; Biopolymer: Bio; Humic substance: HS; Building blocks: BB; Low molecular weight: LMW acids, LMW neutrals.

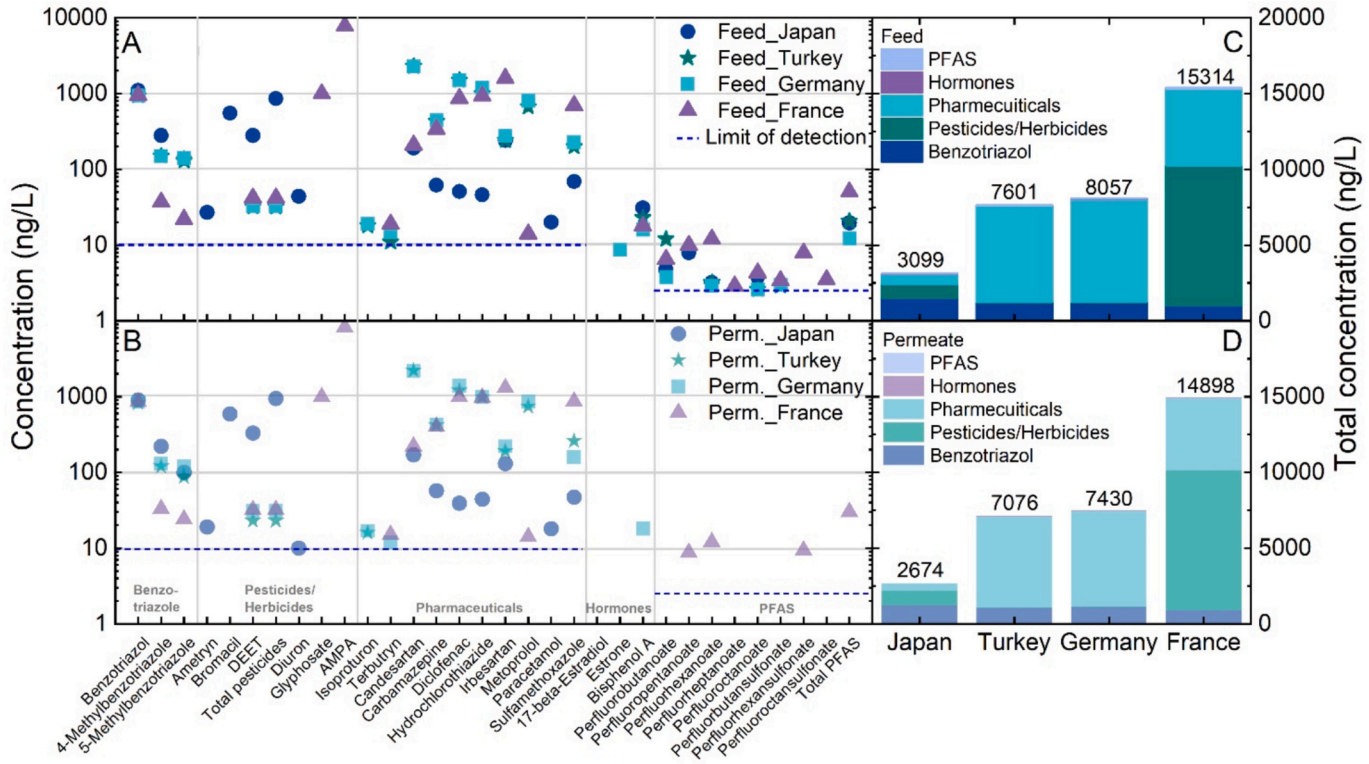

Fig. 9. The concentration of micropollutants in (A) feed, (B) permeate solutions and (C, D) total concentration. Permeate volume 1 L for Germany and France water samples, permeate volume 700 mL for Japan and Turkey water samples. F-M3 (SWCNT, 2.1 g/m^2), 160 ± 16 L/m^2.h, all feed samples were spiked with 100 ng/L radiolabeled E2. The limit of detection of estradiol and estrone is 0.2 ng/L.

and a larger permeate volume (700 mL) was obtained for micropollutant analysis.

3.7. Micropollutant removal with the interference of MBR matrix using composite membrane

To assess the removal of other micropollutants and their competition for adsorption sites, water samples were analyzed using standard analytical methods. Given the limited availability of MBR effluents (1 L from Japan and Turkey, and 4 L from Germany and France), 700 mL of permeate was collected for the experiments of Japan and Turkey, while 1 L was collected for the experiments of Germany and France.

Several micropollutants were detected at high concentrations, ranging from 1000 ng/L (for instance, benzotriazole, glyphosate, and various pharmaceuticals) to 15,000 ng/L (aminomethylphosphonic acid AMPA in the French water sample), exceeding the spiked E2 concentration (100 ng/L) by 1–2 orders of magnitude. Other micropollutants were present at lower but significant concentrations, including 10–100 ng/L of various pesticides and pharmaceuticals, and 2–11 ng/L of PFAS. BPA, used for producing polycarbonates, has hormone-like properties [150] and was present in all samples at concentrations of approximately 20 ng/L. In Fig. 9 C, it is obvious that the concentrations of micropollutants were lower in Japan. It might be attributed to the fact that the Soseigawa Wastewater Treatment Center is connected to a combined sewer system, where the sewage and stormwater are collected, leading to a dilution of micropollutants in wastewater influent [151,152].

The high micropollutant contents in all four MBR effluent samples indicated that MBR was ineffective in fully eliminating micropollutants from polished wastewater, although the concentrations in the influent were not surveyed in this work. The detected PFAS in water samples resisted biodegradation in activated sludge within MBR systems due to their strong carbon–fluorine bonds [153]. Yu et al. reported that MBR treatment removed less than 7 % of perfluorinated compounds, whereas PAC dosing achieved 90 % removal [154].

When considering the treatment using the SWCNT composite, analysis of feed and permeate concentrations in Fig. 9 A, B, revealed no significant differences for benzotriazole, pesticides, herbicides, and pharmaceuticals. In contrast, diuron and BPA exhibited substantial removal, with concentrations decreasing to below 10 ng/L. BPA strongly resembles steroid hormones in structure and can bind to SWCNTs similarly to E2 [155–157]. PFAS concentrations were reduced in all permeates, indicating that feed-side deposition effectively removed PFAS. This removal can be attributed to adsorption by both the membrane material and SWCNTs [158–160]. The low removal of these micropollutants can be attributed to their low affinity for adsorption by SWCNTs, either as their own intrinsic properties or when they are complexed with effluent organic matter, at least within an HRT of 20 milliseconds. The limited performance of the composite membranes indicates that adsorption is not suitable for all micropollutant types.

4. Conclusions

This study demonstrates a potential quaternary treatment for micropollutant removal, in which a feed-side deposition membrane was evaluated for the removal of steroid hormone (17β-estradiol, E2) micropollutants in synthetic background water and MBR effluents following the polishing stage.

Two methods for incorporating SWCNTs—permeate-side and feed-side deposition—were thoroughly examined for E2 removal. In synthetic water, membranes with feed-side SWCNT deposition demonstrated superior E2 removal performance compared to those employing permeate-side deposition. Additionally, SWCNT loading and flux emerged as two major limiting factors for E2 adsorption. A loading of 0.5 g/m^2 SWCNT significantly improved E2 removal from 20 to 85 %, with E2 adsorbed increasing from 2 to 5 ng/cm^2.

A wide range of micropollutants was detected in the effluent, and no significant removal was achieved for a number of these using feed-side deposition. However, several micropollutants, including BPA, were removed, as BPA can compete directly with natural steroid hormone micropollutants for adsorption sites. Indirect competition from organic matter appeared to contribute to the reduced removal of E2 in MBR effluent matrices, as E2 was partitioned to the organic matter, forming complexes with lower affinity for SWCNTs, which were transported through the membrane.

While a SWCNT composite nanofiber membrane with higher SWCNT loading, in conjunction with a membrane featuring a molecular weight cutoff of ≤10 kDa for organic matter screening, can effectively reduce micropollutant–organic matter interactions and enhance the availability of adsorption sites following MBR treatment. The SWCNTs serve as model adsorbents with high adsorption kinetics and adsorption capacity for process evaluation, as results will be transferable to other adsorbent materials that may be more suitable or more ready for industrial application. However, it is unlikely that such a composite membrane will be able to concurrently remove all micropollutants to a significant or required level, which is a reality check for the development of novel materials. Potential future research directions could involve the incorporation of alternative adsorbents targeting specific micropollutants on the permeate side of the UF membrane and focus more on the interplay of effluent organic matter, micropollutants, and adsorbents, as well as the shielding effect of the UF membrane.

CRediT authorship contribution statement

Han-Ya Lin: Writing – original draft, Visualization, Validation, Methodology, Investigation, Formal analysis, Data curation, Conceptualization. **Minh N. Nguyen:** Writing – review & editing, Validation, Methodology, Investigation, Data curation, Conceptualization. **Andrea I. Schäfer:** Writing – review & editing, Supervision, Resources, Project administration, Methodology, Funding acquisition, Conceptualization.

Declaration of competing interest

The authors declare that they have no known competing financial interests or personal relationships that could have appeared to influence the work reported in this paper.

Acknowledgements

The authors acknowledge the financial support from the Helmholtz Recruitment Initiative for the IAMT funding, as well as the Bundesministerium für Bildung und Forschung (BMBF) “RealMethod” project (No. 01DR20011) for project funding through collaboration with Hokkaido University (HU, Japan), University of Poitiers (France), and Istanbul Technical University (ITÜ, Turkey). Katsuki Kimura (HU) and Kotaro Oikawa (Sapporo Sewerage and River Bureau, Soseigawa Water Treatment Center), Benoit Teychene (University of Poitiers), Emma Boissiere (Institute of Filtration and Separation Techniques, IFTS-SLS), Thomas Wintgens (RWTH Aachen University), and Mehmet Emin Pasaoglu (MEMTEK, Istanbul Technical University) are appreciated for their provision of MBR effluents and WWTP information. Rabia Ardıç (MEMTEK, Istanbul Technical University) is appreciated for the provision of PES pristine membranes, supervised by Borte Kose-Mutlu and Ismail Koyuncu (ITÜ) with additional funding by TÜBİTAK (The Scientific and Technological Research Council of Turkey) under Project No. 119N019 to the Turkish partners. Katsuki Kimura (Hokkaido University) is appreciated for providing comments on the manuscript. Justine Nyarige (KIT-IMT) provided SEM images, at KIT-IAMT Francis Adu-Boahene carried out the IC analysis, while Youssef-Amine Boussouga operated the ICP-MS. Bryce S. Richards (KIT-IMT) led the collaboration on the Baden-Württemberg project SPheRe (21-6221.-AFR-2/30) project that funded the micropollutant analysis at TZW. Open access funding was enabled by Project DEAL.

Appendix A. Supplementary data

Supplementary data to this article can be found online at https://doi.org/10.1016/j.cej.2025.170335.

Data availability

Data will be made available on request.

References

[1] N.H. Tran, M. Reinhard, K.Y.-H. Gin, Occurrence and fate of emerging contaminants in municipal wastewater treatment plants from different geographical regions–A review, Water Res. 133 (2018) 182–207.
[2] Z. Tang, Z.-h. Liu, H. Wang, Z. Dang, H. Yin, Y. Zhou, Y. Liu, Trace determination of eleven natural estrogens and insights from their occurrence in a municipal wastewater treatment plant and river water, Water Res. 182 (2020) 115976.
[3] N. Sutaswiriya, S. Homklin, T. Kreetachat, P. Vaithanomsat, N. Kreetachat, Monitoring estrogen and androgen residues from livestock farms in Phayao Lake, Thailand, Environ. Monit. Assess. 193 (12) (2021) 812.
[4] D. Nasuhoglu, D. Berk, V. Yargeau, Photocatalytic removal of 17α-ethinylestradiol (EE2) and levonorgestrel (LNG) from contraceptive pill manufacturing plant wastewater under UVC radiation, Chem. Eng. J. 185-186 (2012) 52–60.
[5] B. Almazrouei, D. Islayem, F. Alskafi, M.K. Catacutan, R. Amna, S. Nasrat, B. Sizirici, I. Yildiz, Steroid hormones in wastewater: sources, treatments, environmental risks, and regulations, Emerg. Contam. 9 (2) (2023) 100210.
[6] B.E. Henderson, H.S. Feigelson, Hormonal carcinogenesis, Carcinogenesis 21 (3) (2000) 427–433.
[7] E. Diamanti-Kandarakis, J.P. Bourguignon, L.C. Giudice, R. Hauser, G.S. Prins, A. M. Soto, R.T. Zoeller, A.C. Gore, Endocrine-disrupting chemicals: an Endocrine Society scientific statement, Endocr. Rev. 30 (4) (2009) 293–342.
[8] Y. Yang, X. Zhang, J. Jiang, J. Han, W. Li, X. Li, K.M. Yee Leung, S.A. Snyder, P.J. J. Alvarez, Which micropollutants in water environments deserve more attention globally? Environ. Sci. Technol. 56 (1) (2022) 13–29.
[9] European Commission, Proposal for a Directive of the European Parliament and of the Council Amending Directives 2000/60/EC and 2008/105/EC as Regards Priority Substances in the Field of Water Policy, 2011.
[10] European Commission, Proposal for a Directive of the European Parliament and of the Council Amending Directive 2000/60/EC Establishing a Framework for Community Action in the Field of Water Policy, Directive 2006/118/EC on the Protection of Groundwater against Pollution and Deterioration and Directive 2008/105/EC on Environmental Quality Standards in the Field of Water Policy, 2022.
[11] S. Al-Asheh, M. Bagheri, A. Aidan, Membrane bioreactor for wastewater treatment: a review, Case Stud. Chem. Environ. Eng. 4 (2021) 100109.
[12] W. Liu, X. Song, Z. Na, G. Li, W. Luo, Strategies to enhance micropollutant removal from wastewater by membrane bioreactors: recent advances and future perspectives, Bioresour. Technol. 344 (2022) 126322.
[13] M. Taheran, S.K. Brar, M. Verma, R.Y. Surampalli, T.C. Zhang, J.R. Valero, Membrane processes for removal of pharmaceutically active compounds (PhACs) from water and wastewaters, Sci. Total Environ. 547 (2016) 60–77.
[14] C. Grandclément, I. Seyssiecq, A. Piram, P. Wong-Wah-Chung, G. Vanot, N. Tiliacos, N. Roche, P. Doumenq, From the conventional biological wastewater treatment to hybrid processes, the evaluation of organic micropollutant removal: a review, Water Res. 111 (2017) 297–317.
[15] S. Wang, X. Ma, Y. Liu, X. Yi, G. Du, J. Li, Fate of antibiotics, antibiotic-resistant bacteria, and cell-free antibiotic-resistant genes in full-scale membrane bioreactor wastewater treatment plants, Bioresour. Technol. 302 (2020) 122825.
[16] T. Leiviskä, S. Risteelä, Analysis of pharmaceuticals, hormones and bacterial communities in a municipal wastewater treatment plant – comparison of parallel full-scale membrane bioreactor and activated sludge systems, Environ. Pollut. 292 (2022) 118433.
[17] J. Guo, S. Qiu, L. Dai, L. Zhang, L. Meng, M. Liu, H. Yao, The occurrence and removal of steroid estrogens in a full-scale anaerobic/anoxic/aerobic-membrane bioreactor process and the implication of the bacterial community dynamics, J. Environ. Chem. Eng. 10 (2) (2022) 107294.
[18] W. Ben, B. Zhu, X. Yuan, Y. Zhang, M. Yang, Z. Qiang, Occurrence, removal and risk of organic micropollutants in wastewater treatment plants across China: comparison of wastewater treatment processes, Water Res. 130 (2018) 38–46.
[19] A. Ofrydopoulou, C. Nannou, E. Evgenidou, A. Christodoulou, D. Lambropoulou, Assessment of a wide array of organic micropollutants of emerging concern in wastewater treatment plants in Greece: occurrence, removals, mass loading and potential risks, Sci. Total Environ. 802 (2022) 149860.
[20] European Commission, Proposal for a Directive of the European Parliament and of the Council Concerning Urban Wastewater Treatment (Recast), 2022.
[21] A. Sonune, R. Ghate, Developments in wastewater treatment methods, Desalination 167 (2004) 55–63.
[22] K. Kimura, G. Amy, J.E. Drewes, T. Heberer, T.-U. Kim, Y. Watanabe, Rejection of organic micropollutants (disinfection by-products, endocrine disrupting compounds, and pharmaceutically active compounds) by NF/RO membranes, J. Membr. Sci. 227 (1) (2003) 113–121.
[23] Y. Yoon, P. Westerhoff, S.A. Snyder, E.C. Wert, Nanofiltration and ultrafiltration of endocrine disrupting compounds, pharmaceuticals and personal care products, J. Membr. Sci. 270 (1) (2006) 88–100.
[24] L.D. Nghiem, S.A. I., M., Elimelech, Nanofiltration of hormone mimicking trace organic contaminants, Sep. Sci. Technol. 40 (13) (2005) 2633–2649.
[25] B. Van Der Bruggen, C. Vandecasteele, T. Van Gestel, W. Doyen, R. Leysen, A review of pressure-driven membrane processes in wastewater treatment and drinking water production, Environ. Prog. 22 (1) (2003) 46–56.
[26] L.D. Nghiem, A.I. Schäfer, M. Elimelech, Removal of natural hormones by nanofiltration membranes: measurement, modeling, and mechanisms, Environ. Sci. Technol. 38 (6) (2004) 1888–1896.
[27] D.L. Nghiem, A.I. Schäfer, Adsorption and transport of trace contaminant Estrone in NF/RO membranes, Environ. Eng. Sci. 19 (6) (2002) 441–451.
[28] G. Bertanza, M. Papa, R. Pedrazzani, C. Repice, G. Mazzoleni, N. Steimberg, D. Feretti, E. Ceretti, I. Zerbini, EDCs, estrogenicity and genotoxicity reduction in a mixed (domestic+textile) secondary effluent by means of ozonation: a full-scale experience, Sci. Total Environ. 458-460 (2013) 160–168.
[29] D. Gerrity, A.N. Pisarenko, E. Marti, R.A. Trenholm, F. Gerringer, J. Reungoat, E. Dickenson, Nitrosamines in pilot-scale and full-scale wastewater treatment plants with ozonation, Water Res. 72 (2015) 251–261.
[30] M. Bourgin, B. Beck, M. Boehler, E. Borowska, J. Fleiner, E. Salhi, R. Teichler, U. von Gunten, H. Siegrist, C.S. McArdell, Evaluation of a full-scale wastewater treatment plant upgraded with ozonation and biological post-treatments: abatement of micropollutants, formation of transformation products and oxidation by-products, Water Res. 129 (2018) 486–498.
[31] J. Margot, C. Kienle, A. Magnet, M. Weil, L. Rossi, L.F. de Alencastro, C. Abegglen, D. Thonney, N. Chèvre, M. Schärer, D.A. Barry, Treatment of micropollutants in municipal wastewater: ozone or powdered activated carbon? Sci. Total Environ. 461-462 (2013) 480–498.
[32] Deutsche Vereinigung für Wasserwirtschaft Abwasser und Abfall, Kläranlagen mit einer 4. Reinigungsstufe zur gezielten Spurenstoffentfernung in Betrieb. https://de.dwa.de/de/landkarte-4-stufe.html, 2025. (Accessed 20 May 2025).
[33] S. Kundu, N. Karak, Polymeric photocatalytic membrane: an emerging solution for environmental remediation, Chem. Eng. J. 438 (2022) 135575.
[34] S. Mozia, Photocatalytic membrane reactors (PMRs) in water and wastewater treatment. A review, Sep. Purif. Technol. 73 (2) (2010) 71–91.
[35] S. Lotfi, K. Fischer, A. Schulze, A.I. Schäfer, Photocatalytic degradation of steroid hormone micropollutants by TiO2-coated polyethersulfone membranes in a continuous flow-through process, Nat. Nanotechnol. 17 (4) (2022) 417–423.
[36] P. Song, Y. Shi, Y. Cai, W. Jiang, X. Fang, X. Ma, L. Sun, D. Liu, S. Liu, X. Wang, C. Lv, W. Duan, T. Kong, Y. Xiong, Integration of three-dimensional printed flow-through photoreactor with z-scheme photocatalytic membrane for sunlight-drivable micropollutant removal from water, ACS Mater. Lett. 7 (2) (2025) 585–594.
[37] R. Lyubimenko, O.I. Gutierrez Cardenas, A. Turshatov, B.S. Richards, A.I. Schäfer, Photodegradation of steroid-hormone micropollutants in a flow-through membrane reactor coated with Pd(II)-porphyrin, Appl. Catal. B Environ. 291 (2021) 120097.
[38] Z. Li, R. Dai, B. Yang, M. Chen, X. Wang, Z. Wang, An electrochemical membrane biofilm reactor for removing sulfonamides from wastewater and suppressing antibiotic resistance development: performance and mechanisms, J. Hazard. Mater. 404 (2021) 124198.
[39] M. Sun, X. Wang, L.R. Winter, Y. Zhao, W. Ma, T. Hedtke, J.-H. Kim, M. Elimelech, Electrified membranes for water treatment applications, ACS ES&T Eng. 1 (4) (2021) 725–752.
[40] S. Liu, D. Jassby, D. Mandler, A.I. Schäfer, Differentiation of adsorption and degradation in steroid hormone micropollutants removal using electrochemical carbon nanotube membrane, Nat. Commun. 15 (1) (2024) 9524.
[41] Y. Wolf, S. Oster, A. Shuliakevich, I. Brückner, R. Dolny, V. Linnemann, J. Pinnekamp, H. Hollert, S. Schiwy, Improvement of wastewater and water quality via a full-scale ozonation plant? – a comprehensive analysis of the endocrine potential using effect-based methods, Sci. Total Environ. 803 (2022) 149756.
[42] E. Worch, Adsorption Technology in Water Treatment, De Gruyter, Berlin, 2012.
[43] Kompetenzzentrum Spurenstoffe Baden-Württemberg, Kläranlagen zur Spurenstoffelimination. https://koms-bw.de/anlagen/, 2025. Accessed 12/02 2024.
[44] M. Evers, R.-L. Lange, E. Heinz, M. Wichern, Simultaneous powdered activated carbon dosage for micropollutant removal on a municipal wastewater treatment plant compared to the efficiency of a post treatment stage, J. Water Process Eng. 47 (2022) 102755.
[45] M. Campinas, R.M.C. Viegas, C.M.M. Almeida, A. Martins, C. Silva, E. Mesquita, M.R. Coelho, S. Silva, V.V. Cardoso, M.J. Benoliel, M.J. Rosa, Powdered activated carbon full-scale addition to the activated sludge reactor of a municipal wastewater treatment plant: pharmaceutical compounds control and overall impact on the process, J. Water Process Eng. 49 (2022) 102975.
[46] F. Esmaeeli, S.A. Gorbanian, N. Moazezi, Removal of estradiol valerate and progesterone using powdered and granular activated carbon from aqueous solutions, Int. J. Environ. Res. Public Health 11 (5) (2017) 695–705.
[47] R. Mailler, J. Gasperi, Y. Coquet, A. Buleté, E. Vulliet, S. Deshayes, S. Zedek, C. Mirande-Bret, V. Eudes, A. Bressy, E. Caupos, R. Moilleron, G. Chebbo, V. Rocher, Removal of a wide range of emerging pollutants from wastewater treatment plant discharges by micro-grain activated carbon in fluidized bed as tertiary treatment at large pilot scale, Sci. Total Environ. 542 (2016) 983–996.
[48] M. Tagliavini, P.G. Weidler, C. Njel, J. Pohl, D. Richter, B. Böhringer, A.I. Schäfer, Polymer-based spherical activated carbon – ultrafiltration (UF-PBSAC) for the

adsorption of steroid hormones from water: material characteristics and process configuration, Water Res. 185 (2020) 116249.
[49] J. Wolters, M. Tagliavini, A.I. Schäfer, Removal of steroid hormone micropollutants by UF-PBSAC composite in presence of organic matter, J. Membr. Sci. 592 (2019) 117315.
[50] A. Mudhoo, D. Mohan, C.U. Pittman, G. Sharma, M. Sillanpää, Adsorbents for real-scale water remediation: gaps and the road forward, J. Environ. Chem. Eng. 9 (4) (2021) 105380.
[51] X. Huang, M. Auffan, M.J. Eckelman, M. Elimelech, J.-H. Kim, J. Rose, K. Zuo, Q. Li, P.J.J. Alvarez, Trends, risks and opportunities in environmental nanotechnology, Nat. Rev. Earth Environ. 5 (8) (2024) 572–587.
[52] M.N. Nguyen, P.G. Weidler, R. Schwaiger, A.I. Schäfer, Interactions between carbon-based nanoparticles and steroid hormone micropollutants in water, J. Hazard. Mater. 402 (2021) 122929.
[53] L. Jiang, Y. Liu, S. Liu, G. Zeng, X. Hu, X. Hu, Z. Guo, X. Tan, L. Wang, Z. Wu, Adsorption of estrogen contaminants by graphene nanomaterials under natural organic matter preloading: comparison to carbon nanotube, biochar, and activated carbon, Environ. Sci. Technol. 51 (11) (2017) 6352–6359.
[54] S. Li, T. De Silva, I. Arsano, D. Gallaba, R. Karunanithy, M. Wasala, X. Zhang, P. Sivakumar, A. Migone, M. Tsige, X. Ma, S. Talapatra, High adsorption of benzoic acid on single walled carbon nanotube bundles, Sci. Rep. 10 (1) (2020) 10013.
[55] W. Kulcke, A. Knabbe, G. Brunner, Characterization of a microfiltration membrane by use of residence time distribution, J. Membr. Sci. 161 (1) (1999) 263–273.
[56] M.N. Nguyen, R. Hérvas-Martínez, A.I. Schäfer, Organic matter interference with steroid hormone removal by single-walled carbon nanotubes – ultrafiltration composite membrane, Water Res. 199 (2021) 117148.
[57] Y. Wang, J. Zhu, H. Huang, H.-H. Cho, Carbon nanotube composite membranes for microfiltration of pharmaceuticals and personal care products: capabilities and potential mechanisms, J. Membr. Sci. 479 (2015) 165–174.
[58] M. Baratta, A.V. Nezhdanov, A.I. Mashin, F.P. Nicoletta, G. De Filpo, Carbon nanotubes buckypapers: a new frontier in wastewater treatment technology, Sci. Total Environ. 924 (2024) 171578.
[59] R. Das, B.F. Leo, F. Murphy, The toxic truth about carbon nanotubes in water purification: a perspective view, Nanoscale Res. Lett. 13 (1) (2018) 183.
[60] A. Freixa, V. Acuña, J. Sanchís, M. Farré, D. Barceló, S. Sabater, Ecotoxicological effects of carbon based nanomaterials in aquatic organisms, Sci. Total Environ. 619-620 (2018) 328–337.
[61] Y. Zhu, X. Liu, Y. Hu, R. Wang, M. Chen, J. Wu, Y. Wang, S. Kang, Y. Sun, M. Zhu, Behavior, remediation effect and toxicity of nanomaterials in water environments, Environ. Res. 174 (2019) 54–60.
[62] E. Cruces, A.C. Barrios, Y.P. Cahue, B. Januszewski, L.M. Gilbertson, F. Perreault, Similar toxicity mechanisms between graphene oxide and oxidized multi-walled carbon nanotubes in Microcystis aeruginosa, Chemosphere 265 (2021) 129137.
[63] T.W.K. FraseR, H.C. Reinardy, B.J. Shaw, T.B. Henry, R.D. Handy, Dietary toxicity of single-walled carbon nanotubes and fullerenes (C60) in rainbow trout (Oncorhynchus mykiss), Nanotoxicology 5 (1) (2011) 98–108.
[64] C.J. Smith, B.J. Shaw, R.D. Handy, Toxicity of single walled carbon nanotubes to rainbow trout, (*Oncorhynchus mykiss*): respiratory toxicity, organ pathologies, and other physiological effects, Aquat. Toxicol. 82 (2) (2007) 94–109.
[65] D. Boyle, J.E. Fox, J.M. Akerman, K.A. Sloman, T.B. Henry, R.D. Handy, Minimal effects of waterborne exposure to single-walled carbon nanotubes on behaviour and physiology of juvenile rainbow trout (Oncorhynchus mykiss), Aquat. Toxicol. 146 (2014) 154–164.
[66] F. Gottschalk, T. Sonderer, R.W. Scholz, B. Nowack, Modeled environmental concentrations of engineered nanomaterials (TiO_2, ZnO, ag, CNT, fullerenes) for different regions, Environ. Sci. Technol. 43 (24) (2009) 9216–9222.
[67] T.Y. Sun, F. Gottschalk, K. Hungerbühler, B. Nowack, Comprehensive probabilistic modelling of environmental emissions of engineered nanomaterials, Environ. Pollut. 185 (2014) 69–76.
[68] E.J. Petersen, L. Zhang, N.T. Mattison, D.M. O'Carroll, A.J. Whelton, N. Uddin, T. Nguyen, Q. Huang, T.B. Henry, R.D. Holbrook, K.L. Chen, Potential release pathways, environmental fate, and ecological risks of carbon nanotubes, Environ. Sci. Technol. 45 (23) (2011) 9837–9856.
[69] E.J. Petersen, D.X. Flores-Cervantes, T.D. Bucheli, L.C.C. Elliott, J.A. Fagan, A. Gogos, S. Hanna, R. Kägi, E. Mansfield, A.R.M. Bustos, D.L. Plata, V. Reipa, P. Westerhoff, M.R. Winchester, Quantification of carbon nanotubes in environmental matrices: current capabilities, case studies, and future prospects, Environ. Sci. Technol. 50 (9) (2016) 4587–4605.
[70] F.-f. Ma, D. Zhang, T. Huang, N. Zhang, Y. Wang, Ultrasonication-assisted deposition of graphene oxide on electrospun poly(vinylidene fluoride) membrane and the adsorption behavior, Chem. Eng. J. 358 (2019) 1065–1073.
[71] L. Xie, Y. Shu, Y. Hu, J. Cheng, Y. Chen, SWNTs-PAN/TPU/PANI composite electrospun nanofiber membrane for point-of-use efficient electrochemical disinfection: new strategy of CNT disinfection, Chemosphere 251 (2020) 126286.
[72] X. Cheng, W. Zhou, P. Li, Z. Ren, D. Wu, C. Luo, X. Tang, J. Wang, H. Liang, Improving ultrafiltration membrane performance with pre-deposited carbon nanotubes/nanofibers layers for drinking water treatment, Chemosphere 234 (2019) 545–557.
[73] J.-C. Han, Y.-K. Zhu, L.-F. Wang, Y. Mu, G.-G. Feng, K.-Q. Liu, C.-H. Tong, Z.-X. Yu, Modification of regenerated cellulose ultrafiltration membranes with multi-walled carbon nanotubes for enhanced antifouling ability: field test and mechanism study, Sci. Total Environ. 780 (2021) 146657.
[74] Y. Wang, Y. Liu, Y. Yu, H. Huang, Influence of CNT-rGO composite structures on their permeability and selectivity for membrane water treatment, J. Membr. Sci. 551 (2018) 326–332.
[75] W. Zhang, J. Mo, W. Liang, X. Du, Carbon nanotube-adsorptive dynamic membrane (CNT-ADM) for water purification, J. Water Process Eng. 51 (2023) 103433.
[76] G. Kaminska, J. Bohdziewicz, J.I. Calvo, P. Prádanos, L. Palacio, A. Hernández, Fabrication and characterization of polyethersulfone nanocomposite membranes for the removal of endocrine disrupting micropollutants from wastewater. Mechanisms and performance, J. Membr. Sci. 493 (2015) 66–79.
[77] Y. Zhan, X. Wan, S. He, Q. Yang, Y. He, Design of durable and efficient poly (arylene ether nitrile)/bioinspired polydopamine coated graphene oxide nanofibrous composite membrane for anionic dyes separation, Chem. Eng. J. 333 (2018) 132–145.
[78] M.N. Nguyen, P.B. Trinh, C.J. Burkhardt, A.I. Schäfer, Incorporation of single-walled carbon nanotubes in ultrafiltration support structure for the removal of steroid hormone micropollutants, Sep. Purif. Technol. 264 (2021) 118405.
[79] K.M. Dobosz, C.A. Kuo-Leblanc, M.E. Bowden, J.D. Schiffman, Robust, small diameter hydrophilic nanofibers improve the flux of ultrafiltration membranes, Ind. Eng. Chem. Res. 60 (25) (2021) 9179–9188.
[80] S.-N. Nam, G. Amy, Differentiation of wastewater effluent organic matter (EfOM) from natural organic matter (NOM) using multiple analytical techniques, Water Sci. Technol. 57 (7) (2008) 1009–1015.
[81] H.K. Shon, A. V., A. S., Snyder, Effluent organic matter (EfOM) in wastewater: constituents, effects, and treatment, Crit. Rev. Environ. Sci. Technol. 36 (4) (2006) 327–374.
[82] C. Jarusutthirak, G. Amy, Understanding soluble microbial products (SMP) as a component of effluent organic matter (EfOM), Water Res. 41 (12) (2007) 2787–2793.
[83] Y. Chun, T. Hua, A. Anantharaman, J.W. Chew, N. Cai, M. Benjamin, R. Wang, Organic matter removal from a membrane bioreactor effluent for reverse osmosis fouling mitigation by microgranular adsorptive filtration system, Desalination 506 (2021) 115016.
[84] Z. Xue, Z. Lv, C. Liu, X. Yang, S. Yu, L. Li, Chromatographic and spectroscopic comparison of dissolved organic matter variation in anaerobic-anoxic-oxic process with tertiary filtration and membrane bioreactor, J. Water Process Eng. 47 (2022) 102693.
[85] B.G. Choi, J. Cho, K.G. Song, S.K. Maeng, Correlation between effluent organic matter characteristics and membrane fouling in a membrane bioreactor using advanced organic matter characterization tools, Desalination 309 (2013) 74–83.
[86] M. Engel, B. Chefetz, Removal of triazine-based pollutants from water by carbon nanotubes: impact of dissolved organic matter (DOM) and solution chemistry, Water Res. 106 (2016) 146–154.
[87] M. Engel, B. Chefetz, The missing link between carbon nanotubes, dissolved organic matter and organic pollutants, Adv. Colloid Interf. Sci. 271 (2019) 101993.
[88] P.A. Neale, A.I. Schäfer, Quantification of solute–solute interactions in steroidal hormone removal by ultrafiltration membranes, Sep. Purif. Technol. 90 (2012) 31–38.
[89] A.I. Schäfer, A.G. Fane, T.D. Waite, Cost factors and chemical pretreatment effects in the membrane filtration of waters containing natural organic matter, Water Res. 35 (6) (2000) 1509–1517.
[90] S. Meylan, F. Hammes, J. Traber, E. Salhi, U. von Gunten, W. Pronk, Permeability of low molecular weight organics through nanofiltration membranes, Water Res. 41 (2007) 3968–3976.
[91] Y. Zha, Y. Wang, S. Liu, S. Liu, Y. Yang, H. Jiang, Y. Zhang, L. Qi, H. Wang, Adsorption characteristics of organics in the effluent of ultra-short SRT wastewater treatment by single-walled, multi-walled, and graphitized multi-walled carbon nanotubes, Sci. Rep. 8 (1) (2018) 17245.
[92] K. Yang, B. Xing, Adsorption of fulvic acid by carbon nanotubes from water, Environ. Pollut. 157 (4) (2009) 1095–1100.
[93] M.E. Pasaoglu, S. Guclu, I. Koyuncu, Polyethersulfone/polyacrylonitrile blended ultrafiltration membranes: preparation, morphology and filtration properties, Water Sci. Technol. 74 (3) (2016) 738–748.
[94] A. Mehta, A.L. Zydney, Permeability and selectivity analysis for ultrafiltration membranes, J. Membr. Sci. 249 (1) (2005) 245–249.
[95] A. Imbrogno, H.Y. Lin, B. Minofar, A.I. Schäfer, Nanofiber composite ultrafiltration membrane functionalized with cross-linked β-cyclodextrin for steroid hormone micropollutant removal, J. Membr. Sci. 691 (2024) 122212.
[96] M. Rahmati Nejad, M. Yousefzadeh, A. Solouk, Electrospun PET/PCL small diameter nanofibrous conduit for biomedical application, Mater. Sci. Eng. C 110 (2020) 110692.
[97] M. Bilal, D. Barceló, H.M.N. Iqbal, Occurrence, environmental fate, ecological issues, and redefining of endocrine disruptive estrogens in water resources, Sci. Total Environ. 800 (2021) 149635.
[98] L. Varticovski, D.A. Stavreva, A. McGowan, R. Raziuddin, G.L. Hager, Endocrine disruptors of sex hormone activities, Mol. Cell. Endocrinol. 539 (2022) 111415.
[99] European Parliament, Commission Implementing Decision (EU) 2022/679 of 19 January 2022 Establishing a Watch List of Substances and Compounds of Concern for Water Intended for Human Consumption as Provided for in Directive (EU) 2020/2184 of the European Parliament and of the Council (Notified under Document C(2022) 142), 2022.
[100] G.-G. Ying, R.S. Kookana, Y.-J. Ru, Occurrence and fate of hormone steroids in the environment, Environ. Int. 28 (6) (2002) 545–551.

[101] M.O. Barbosa, N.F.F. Moreira, A.R. Ribeiro, M.F.R. Pereira, A.M.T. Silva, Occurrence and removal of organic micropollutants: an overview of the watch list of EU decision 2015/495, Water Res. 94 (2016) 257–279.
[102] L.M. Madikizela, S. Ncube, L. Chimuka, Analysis, occurrence and removal of pharmaceuticals in African water resources: a current status, J. Environ. Manag. 253 (2020) 109741.
[103] T. Miyoshi, T.P. Nguyen, T. Tsumuraya, K. Kimura, Y. Watanabe, Energy consumption in a baffled membrane bioreactor (B-MBR): estimation based on long-term continuous operation, Water Sci. Technol. 80 (6) (2019) 1011–1021.
[104] K. Kimura, R. Nishisako, T. Miyoshi, R. Shimada, Y. Watanabe, Baffled membrane bioreactor (BMBR) for efficient nutrient removal from municipal wastewater, Water Res. 42 (3) (2008) 625–632.
[105] S. Basu, S.K. Singh, P.K. Tewari, V.S. Batra, M. Balakrishnan, Treatment of nitrate-rich water in a baffled membrane bioreactor (BMBR) employing waste derived materials, J. Environ. Manag. 146 (2014) 16–21.
[106] S. Lyko, T. Wintgens, D. Al-Halbouni, S. Baumgarten, D. Tacke, K. Drensla, A. Janot, W. Dott, J. Pinnekamp, T. Melin, Long-term monitoring of a full-scale municipal membrane bioreactor—characterisation of foulants and operational performance, J. Membr. Sci. 317 (1) (2008) 78–87.
[107] Agglomération d'Agen, Agglomération d'Agen – assainissement 2019 rapport annuel du delegataire. https://www.agglo-agen.net/fileadmin/user_upload_agglo/kiosque/Assainissement-rapport-annuel-delegataire-2019.pdf, 2019. (Accessed 2 December 2024).
[108] Polymem, Gestion de l'eau pour les infrastructures de défense en métropole et outre-mer, 2024. https://aqua-valley.com/wp-content/uploads/2024/06/23-Polymem.pdf. (Accessed 12/02 2024).
[109] M.E. Pasaoglu, Personal communication: Flow diagram of Ağva advanced biological WWTP, in: H.-Y. Lin (Ed.) 2024.
[110] MEMSIS Environmental Technologies, İSKİ AĞVA wastewater treatment plant – 8000 m3/day, 2024. https://www.en.memsis.com.tr/referans/iski-agva-waste water-treatment-plant/. (Accessed 12/02 2024).
[111] M.Ç. Teknolojileri, GENMBR® Membrane bioreactor modules, 2024. https://www.memsis.com.tr/urunler/genmbr-membran-biyoreaktor-modulleri/. (Accessed 12/02 2024).
[112] J.L. Weishaar, G.R. Aiken, B.A. Bergamaschi, M.S. Fram, R. Fujii, K. Mopper, Evaluation of specific ultraviolet absorbance as an indicator of the chemical composition and reactivity of dissolved organic carbon, Environ. Sci. Technol. 37 (20) (2003) 4702–4708.
[113] S.A. Huber, A. Balz, M. Abert, W. Pronk, Characterisation of aquatic humic and non-humic matter with size-exclusion chromatography – organic carbon detection – organic nitrogen detection (LC-OCD-OND), Water Res. 45 (2) (2011) 879–885.
[114] Y. Tang, J. Xu, C. Gao, Ultrafiltration membranes with ultrafast water transport tuned via different substrates, Chem. Eng. J. 303 (2016) 322–330.
[115] H. Wu, H. Zhao, Y. Lin, X. Liu, H. Yao, L. Yu, H. Wang, X. Wang, Fabrication of polysulfone membrane with sponge-like structure by using different non-woven fabrics, Sep. Purif. Technol. 297 (2022) 121553.
[116] M. Ulbricht, W. Ansorge, I. Danielzik, M. König, O. Schuster, Fouling in microfiltration of wine: the influence of the membrane polymer on adsorption of polyphenols and polysaccharides, Sep. Purif. Technol. 68 (3) (2009) 335–342.
[117] Z. Li, X. Luo, Y. Li, Reed rhizome residue-based activated carbon adsorption ultrafiltration membranes for enhanced MB removal, ACS Omega 7 (48) (2022) 43829–43838.
[118] H.Y. Lin, A.I. Schäfer, Adsorption of steroid hormone micropollutant by polyethersulfone ultrafiltration membranes with varying morphology, Sep. Purif. Technol. 354 (2025) 128733.
[119] S. Zhang, T. Shao, S.S.K. Bekaroglu, T. Karanfil, The impacts of aggregation and surface chemistry of carbon nanotubes on the adsorption of synthetic organic compounds, Environ. Sci. Technol. 43 (15) (2009) 5719–5725.
[120] G. Ersan, Y. Kaya, M.S. Ersan, O.G. Apul, T. Karanfil, Adsorption kinetics and aggregation for three classes of carbonaceous adsorbents in the presence of natural organic matter, Chemosphere 229 (2019) 515–524.
[121] I. Langmuir, The adsorption of gases on plane surfaces of glass, mica and platinum, J. Am. Chem. Soc. 40 (9) (1918) 1361–1403.
[122] X. Guo, J. Wang, Comparison of linearization methods for modeling the Langmuir adsorption isotherm, J. Mol. Liq. 296 (2019) 111850.
[123] J. Zhang, M.N. Nguyen, Y. Li, C. Yang, A.I. Schäfer, Steroid hormone micropollutant removal from water with activated carbon fiber-ultrafiltration composite membranes, J. Hazard. Mater. 391 (2020) 122020.
[124] S. Manimegalai, S. Vickram, S.R. Deena, K. Rohini, S. Thanigaivel, S. Manikandan, R. Subbaiya, N. Karmegam, W. Kim, M. Govarthanan, Carbon-based nanomaterial intervention and efficient removal of various contaminants from effluents – a review, Chemosphere 312 (2023) 137319.
[125] Y. Yoon, P. Westerhoff, S.A. Snyder, M. Esparza, HPLC-fluorescence detection and adsorption of bisphenol a, 17β-estradiol, and 17α-ethynyl estradiol on powdered activated carbon, Water Res. 37 (14) (2003) 3530–3537.
[126] S. Lee, J.-W. Lee, S. Kim, P.-K. Park, J.-H. Kim, C.-H. Lee, Removal of 17β-estradiol by powdered activated carbon—Microfiltraion hybrid process: the effect of PAC deposition on membrane surface, J. Membr. Sci. 326 (1) (2009) 84–91.
[127] K.-Y. Song, P.-K. Park, J.-H. Kim, C.-H. Lee, S. Lee, Coupling effect of 17β-estradiol and natural organic matter on the performance of a PAC adsorption/membrane filtration hybrid system, Desalination 237 (1) (2009) 392–399.
[128] M. Fuerhacker, A. Dürauer, A. Jungbauer, Adsorption isotherms of 17β-estradiol on granular activated carbon (GAC), Chemosphere 44 (7) (2001) 1573–1579.
[129] K. Cai, D.H. Phillips, C.T. Elliott, M. Muller, M.-L. Scippo, L. Connolly, Removal of natural hormones in dairy farm wastewater using reactive and sorptive materials, Sci. Total Environ. 461-462 (2013) 1–9.
[130] M. Tagliavini, F. Engel, P.G. Weidler, T. Scherer, A.I. Schäfer, Adsorption of steroid micropollutants on polymer-based spherical activated carbon (PBSAC), J. Hazard. Mater. 337 (2017) 126–137.
[131] M. Guedes Maniero, D. Maia Bila, M. Dezotti, Degradation and estrogenic activity removal of 17β-estradiol and 17α-ethinylestradiol by ozonation and O3/H2O2, Sci. Total Environ. 407 (1) (2008) 105–115.
[132] Y. Lin, Z. Peng, X. Zhang, Ozonation of estrone, estradiol, diethylstilbestrol in waters, Desalination 249 (1) (2009) 235–240.
[133] D. Bila, A.F. Montalvão, D.d.A. Azevedo, M. Dezotti, Estrogenic activity removal of 17β-estradiol by ozonation and identification of by-products, Chemosphere 69 (5) (2007) 736–746.
[134] D.P. Grover, J.L. Zhou, P.E. Frickers, J.W. Readman, Improved removal of estrogenic and pharmaceutical compounds in sewage effluent by full scale granular activated carbon: impact on receiving river water, J. Hazard. Mater. 185 (2) (2011) 1005–1011.
[135] R. Guillossou, J. Le Roux, R. Mailler, C.S. Pereira-Derome, G. Varrault, A. Bressy, E. Vulliet, C. Morlay, F. Nauleau, V. Rocher, J. Gasperi, Influence of dissolved organic matter on the removal of 12 organic micropollutants from wastewater effluent by powdered activated carbon adsorption, Water Res. 172 (2020) 115487.
[136] F.C. Kent, J. Citulski, K. Farahbakhsh, Water reclamation using membranes: permeate water quality comparison of MBR and tertiary membrane filtration, Desalination 274 (1) (2011) 237–245.
[137] N.A.A. Qasem, R.H. Mohammed, D.U. Lawal, Removal of heavy metal ions from wastewater: a comprehensive and critical review, NPJ Clean Water. 4 (1) (2021) 36.
[138] C. Tchienkoua, B. Thiodjio Sendja, C.R. Tchenguem Kamto, D. Tchana Kamgne, N.A. Medellin-Castillo, G.J. Labrada-Delgado, J.M. Ndjaka, Sorption of metal elements by single-walled carbon nanotubes and x-ray absorption spectroscopy analysis, Phys Scr 98 (8) (2023) 085901.
[139] J. Adusei-Gyamfi, B. Ouddane, L. Rietveld, J.-P. Cornard, J. Criquet, Natural organic matter-cations complexation and its impact on water treatment: a critical review, Water Res. 160 (2019) 130–147.
[140] Y.-H. Cai, A. Gopalakrishnan, Q. Dong, A.I. Schäfer, Removal of strontium by nanofiltration: role of complexation and speciation of strontium with organic matter, Water Res. 253 (2024) 121241.
[141] C. Jin, Z. Li, A.S. Hursthouse, X. Ding, M. Zhou, J. Chen, B. Li, Manganese oxides mediated dissolve organic matter compositional changes in lake sediment and cadmium binding characteristics, Ecotoxicol. Environ. Saf. 256 (2023) 114916.
[142] F. Zietzschmann, E. Worch, J. Altmann, A.S. Ruhl, A. Sperlich, F. Meinel, M. Jekel, Impact of EfOM size on competition in activated carbon adsorption of organic micro-pollutants from treated wastewater, Water Res. 65 (2014) 297–306.
[143] Q. Wang, R.-L. Mitchell, R. Hofman, J. Yu, M. Yang, L.C. Rietveld, F. Zietzschmann, How properties of low molecular weight model competitors impact organic micropollutant adsorption onto activated carbon at realistically asymmetric concentrations, Water Res. 202 (2021) 117443.
[144] M. Borisover, Y. Laor, N. Bukhanovsky, I. Saadi, Fluorescence-based evidence for adsorptive binding of pyrene to effluent dissolved organic matter, Chemosphere 65 (11) (2006) 1925–1934.
[145] M.M. Puchalski, M.J. Morra, R. Von Wandruszka, Fluorescence quenching of synthetic organic compounds by humic materials, Environ. Sci. Technol. 26 (9) (1992) 1787–1792.
[146] D.A. Backhus, C. Golini, E. Castellanos, Evaluation of fluorescence quenching for assessing the importance of interactions between nonpolar rrganic pollutants and dissolved organic matter, Environ. Sci. Technol. 37 (20) (2003) 4717–4723.
[147] S. Hernandez-Ruiz, L. Abrell, S. Wickramasekara, B. Chefetz, J. Chorover, Quantifying PPCP interaction with dissolved organic matter in aqueous solution: combined use of fluorescence quenching and tandem mass spectrometry, Water Res. 46 (4) (2012) 943–954.
[148] D. Zhang, S. Yang, C. Yang, Y. Chen, R. Hu, Y. Xie, Y. Wang, W. Wang, New insights into the interaction between dissolved organic matter and different types of antibiotics, oxytetracycline and sulfadiazine: multi-spectroscopic methods and density functional theory calculations, Sci. Total Environ. 820 (2022) 153258.
[149] B. Yang, C. Wang, X. Cheng, Y. Zhang, W. Li, J. Wang, Z. Tian, W. Chu, G. V. Korshin, H. Guo, Interactions between the antibiotic tetracycline and humic acid: examination of the binding sites, and effects of complexation on the oxidation of tetracycline, Water Res. 202 (2021) 117379.
[150] S.A. Vogel, Is it safe? BPA and the struggle to define the safety of chemicals, 1 ed., University of California Press2013.
[151] M.A. Launay, U. Dittmer, H. Steinmetz, Organic micropollutants discharged by combined sewer overflows – characterisation of pollutant sources and stormwater-related processes, Water Res. 104 (2016) 82–92.
[152] Y. Luo, W. Guo, H.H. Ngo, L.D. Nghiem, F.I. Hai, J. Zhang, S. Liang, X.C. Wang, A review on the occurrence of micropollutants in the aquatic environment and their fate and removal during wastewater treatment, Sci. Total Environ. 473-474 (2014) 619–641.
[153] A. Podder, A.H.M.A. Sadmani, D. Reinhart, N.-B. Chang, R. Goel, Per and poly-fluoroalkyl substances (PFAS) as a contaminant of emerging concern in surface water: a transboundary review of their occurrences and toxicity effects, J. Hazard. Mater. 419 (2021) 126361.

[154] J. Yu, C. He, X. Liu, J. Wu, Y. Hu, Y. Zhang, Removal of perfluorinated compounds by membrane bioreactor with powdered activated carbon (PAC): adsorption onto sludge and PAC, Desalination 334 (1) (2014) 23–28.
[155] J. Heo, J.R.V. Flora, N. Her, Y.-G. Park, J. Cho, A. Son, Y. Yoon, Removal of bisphenol a and 17β-estradiol in single walled carbon nanotubes–ultrafiltration (SWNTs–UF) membrane systems, Sep. Purif. Technol. 90 (2012) 39–52.
[156] Q. Zaib, I.A. Khan, N.B. Saleh, J.R.V. Flora, Y.-G. Park, Y. Yoon, Removal of bisphenol a and 17β-estradiol by single-walled carbon nanotubes in aqueous solution: adsorption and molecular modeling, Water Air Soil Pollut. 223 (6) (2012) 3281–3293.
[157] B. Pan, D. Lin, H. Mashayekhi, B. Xing, Adsorption and hysteresis of bisphenol a and 17α-ethinyl estradiol on carbon nanomaterials, Environ. Sci. Technol. 42 (15) (2008) 5480–5485.
[158] M. Sörengård, V. Franke, R. Tröger, L. Ahrens, Losses of poly- and perfluoroalkyl substances to syringe filter materials, J. Chromatogr. A 1609 (2020) 460430.
[159] K. He, A. Feerick, H. Jin, J.A. Batista Andrade, M. Duarte Batista, C. Dugan, L. Blaney, Retention of per- and polyfluoroalkyl substances by syringe filters, Environ. Chem. Lett. 22 (4) (2024) 1569–1579.
[160] S. Deng, Q. Zhang, Y. Nie, H. Wei, B. Wang, J. Huang, G. Yu, B. Xing, Sorption mechanisms of perfluorinated compounds on carbon nanotubes, Environ. Pollut. 168 (2012) 138–144.